Published in final edited form as:
J Neurosci. 2008 October 15; 28(42): 10604–10617. doi:10.1523/JNEUROSCI.2709-08.2008.

The stargazin-related protein γ_7 interacts with the mRNA binding protein hnRNP A2 and regulates the stability of specific mRNAs including $Ca_V2.2$

Laurent Ferron, **Anthony Davies**, **Karen M. Page**, **David J. Cox**, **Jerôme Leroy**[†], **Dominic Waithe**, **Adrian J. Butcher**, **Priya Sellaturay**, **Steven Bolsover**, **Wendy S. Pratt**, **Fraser J. Moss**[‡], and **Annette C. Dolphin**[*]
Department of Neuroscience, Physiology and Pharmacology, University College London, London, UK

Abstract

The role(s) of the novel stargazin-like γ-subunit proteins remain controversial. We have shown previously that the neuron-specific γ_7 suppresses the expression of certain calcium channels, particularly $Ca_V2.2$, and is therefore unlikely to operate as a calcium channel subunit. We now show that the effect of γ_7 on $Ca_V2.2$ expression is via an increase in the degradation rate of $Ca_V2.2$ mRNA, and hence a reduction of $Ca_V2.2$ protein level. Furthermore, exogenous expression of γ_7 in PC12 cells also decreased the endogenous $Ca_V2.2$ mRNA level. Conversely, knockdown of endogenous γ_7 with short-hairpin RNAs produced a reciprocal enhancement of $Ca_V2.2$ mRNA stability and an increase in endogenous calcium currents in PC12 cells. Moreover, both endogenous and expressed γ_7 are present on intracellular membranes, rather than the plasma membrane. The cytoplasmic C-terminus of γ_7 is essential for all its effects, and we show that γ_7 binds directly via its C-terminus to a ribonucleoprotein (hnRNP A2), which also binds to a motif in $Ca_V2.2$ mRNA, and is associated with native $Ca_V2.2$ mRNA in PC12 cells. The expression of hnRNP A2 enhances $Ca_V2.2$ I_{Ba} and this enhancement is prevented by a concentration of γ_7 that alone has no effect on I_{Ba}. The effect of γ_7 is selective for certain mRNAs as it had no effect on $\alpha_2\delta$-2 mRNA stability, but it decreased the mRNA stability for the potassium-chloride co-transporter, KCC1, which contains a similar hnRNP A2 binding motif to that in $Ca_V2.2$ mRNA. Our results indicate that γ_7 plays a role in stabilizing $Ca_V2.2$ mRNA.

Keywords

N-type; calcium channel; mRNA stability; gamma7 subunit; hnRNP A2; stargazin

Introduction

Voltage-dependent calcium channels (Ca_V) are hetero-multimers consisting of a pore-forming α_1 subunit, assembled with auxiliary β, $\alpha_2\delta$ and possibly γ subunits (for review see Catterall, 2000; Dolphin, 2003a; Dolphin, 2003b). The role(s) of the γ subunits in relation to calcium channel function remains unclear. The first $Ca_V\gamma$ subunit to be identified was γ_1, which co-purifies with the skeletal muscle calcium channel complex (Jay et al., 1991;

[*]Corresponding author; Laboratory of Cellular and Molecular Neuroscience, Andrew Huxley Building, Department of Pharmacology, University College London, Gower Street, London, WC1E 6BT, UK. Email: a.dolphin@ucl.ac.uk. tel +44 207 679 3276; fax +44 207 679 0042.
[†]Current address: INSERM U-446, Faculté de Pharmacie, F-92296 Châtenay-Malabry, France.
[‡]Current address: Dept. Biology, California Institute of Technology, Pasadena CA 91125, USA.

Europe PMC Funders Author Manuscripts

Powers et al., 1993). In skeletal muscle the γ_1 subunit appears to have a suppressive effect, as γ_1 knockout mice exhibit increased skeletal muscle calcium currents (Freise et al., 2000). Following the identification of stargazin (γ_2) (Letts et al., 1998), subsequent studies have identified six further putative γ subunits (γ_3-γ_8) (Black and Lennon, 1999; Burgess et al., 1999; Klugbauer et al., 2000; Burgess et al., 2001; Moss et al., 2002). However, it is unclear whether any of these novel stargazin-like γ proteins ($\gamma_{2\text{-}8}$) play any role as subunits of voltage-gated calcium channels. All members of this family are thought to possess four transmembrane spanning domains with intracellular N- and C-termini. The γ_2, γ_3, γ_4 and γ_8 subunits form a sub-family exclusively localized to the central nervous system (Letts et al., 1998; Klugbauer et al., 2000; Sharp et al., 2001; Moss et al., 2003) whose interaction and functional modulation of Ca_V channels has been investigated in several studies (Letts et al., 1998; Klugbauer et al., 2000; Sharp et al., 2001; Kang et al., 2001; Rousset et al., 2001; Moss et al., 2003), but which are now thought primarily to represent trafficking proteins for the alpha-amino-3-hydroxyl-5-methyl-4-isoxazolepropionate (AMPA) subtype of glutamate receptors (TARPS) (Tomita et al., 2003; Tomita et al., 2004). However, they might also provide a bridge between calcium channels and AMPA receptors (Kang et al., 2006). Furthermore, γ_7, despite not having a classical C-terminal PDZ binding domain, has also recently been shown to have effects on AMPA receptor trafficking (Kato et al., 2007).

The γ_7 and γ_5 proteins are predicted to represent a distinct sub-family of stargazin-related proteins (Burgess et al., 2001; Chu et al., 2001; Moss et al., 2002), with extremely low sequence identity to γ_1 and approximately 25% identity to γ_2, mainly in the transmembrane domains. We showed that co-expression of the γ_7 subunit with $Ca_V2.2$ almost abolished the functional expression and markedly suppressed the level of $Ca_V2.2$ α_1 subunit protein (Moss et al., 2002). It also had smaller suppressive effects on $Ca_V2.1$ and $Ca_V1.2$ currents (Moss et al., 2002). Our conclusion was that γ_7 was not a subunit of these calcium channels. Nevertheless, because of the marked effect of γ_7 on calcium channel expression, and since both N-type calcium channels and γ_7 are specifically expressed in neuronal tissue, we have now examined the mechanism of action of γ_7 in order to probe its physiological function.

The present results indicate that γ_7 is involved in regulating the stability of specific mRNAs, including $Ca_V2.2$. We propose that the mechanism may involve γ_7 sequestering a specific mRNA binding protein, thus compromising the stability of $Ca_V2.2$ mRNA.

Materials and Methods

cDNA constructs

The following cDNAs were used: $Ca_V2.2$ (D14157) and $Ca_V2.2$ δ3′UTR, $Ca_V3.1$ (AF027984), β1b (X61394, Dr. T. P. Snutch), $\alpha_2\delta$-2 (AF247139, common brain splice variant), γ_7 (NM031896), mut-3b Green Fluorescent Protein (GFP, M62653, except S72A and S65G, Dr. T. E. Hughes), mouse KCC1 (AF121118), $K_V3.1b$ (M68880), hnRNP A1 (BC070315) and hnRNP A2-ΔRGG (Nichols et al., 2000). Truncated and tagged γ_7 constructs and HA-tagged hnRNP A2 were generated using standard molecular biological techniques and confirmed by DNA sequencing. All constructs were cloned into the pMT2 expression vector (Swick et al., 1992), except γ_7-HA and γ_7-CFP, hnRNP A2-ΔRGG and KCC1, all of which were in pCDNA3.1, except γ_7-CFP in pECFP-N1, Kv3.1b in pRC-CMV and hnRNP A1 in pCGT7. pDsRed2-ER plasmid was used in some experiments (Clontech).

Short hairpin RNA design and expression plasmid

siSearch (http://sonnhammer.sbc.su.se/databases.html) and Jura (http://jura.wi.mit.edu/siRNAext/) software was used to design 19-nucleotides sequences corresponding to human

and rat γ_7 genes. Databases were searched to ensure that these sequences were not homologous to any other known genes. Rat γ_7 (AF361345) targets: γ_7 96 (5′-CTGGCTGTATATGGAGGAG-3′), γ_7 285 (5′-GACAGTACGCACGGCTACA-3′), γ_7 500 (5′-CTGAGCAATACTTTCACTA-3′). Human γ_7 (AF458897) targets: γ_7 96 (5′-CTGGCTGTACATGGAAGAA-3′), γ_7 285 (5′-GACAGTGCGCACGGCCACC-3′), γ_7 107 (5′-TGGAAGAAGGCACAGTGCT-3′). Then, for each target, 2 oligonucleotides (A and B) were synthesized (Invitrogen, Paisley UK). Oligonucleotide A contains a 5′-overhang (TTTG) for ligation into a *Bpi*I (*Bbs*I) site, the sense and the antisense of these sequences linked by a hairpin loop of 9 bases (TTCAAGAGA (Brummelkamp et al., 2002)), and a TTTTT sequence corresponding to a termination for transcription of small RNAs by RNA polymerase III; oligonucleotide B contains a 5′-overhang (CTAG) for ligation into a *Xba*I site, and 52 nucleotides corresponding to the reverse complement of the last 52 nucleotides of oligonucleotide A. Forward and reverse strands were annealed and subcloned downstream a U6 promoter into pG418-shRNA-Empty linearized with *Xba*I and *Bpi*I. pG418-shRNA-Empty is a pBSII plasmid containing a mouse U6 promoter and a neomycin (G418) resistance cassette. A negative control shRNA, directed against drosophila gene *gnu* (Xu and Shrager, 2005) and a positive control shRNA directed against c-jun (Lingor et al., 2005), were also synthesized. Correct orientation and location of oligonucleotides cloning were confirmed by sequencing the plasmids. Validation of the plasmid in PC12 cells was determined by its ability to knock-down c-jun (see Supplemental Fig. 1).

Antibodies against γ_7

The γ_7 tail polyclonal rabbit Ab raised against the C-terminal peptide YPPAIKYPDHLHIS has been described previously (Moss et al., 2002). A γ_7 loop Ab was also raised against the peptide VASEYFLEPEINLVTEN, in the loop between transmembrane segments 1 and 2 of γ_7. These Abs do not recognize any of the other γ proteins tested (γ_2, γ_3 or γ_4, Supplemental Fig. 2*A*-*C*).

Cell culture and transfection

COS-7 cells were cultured as previously described (Campbell et al., 1995). The tsA 201 cells were cultured in D-MEM with 10% fetal bovine serum (FBS) and 1% L-glutamine. Cells were transfected using either Geneporter (Qbiogene, Harefield, UK) or Fugene6 (Roche Diagnostics, Lewes, UK), with equivalent results. The cDNAs (all at 1 $\mu g.\mu l^{-1}$) for $Ca_V\alpha 1$, $\alpha_2\delta$-2, β1b, γ_7 and GFP when used as a reporter of transfected cells, were mixed in a ratio of 3 : 1.5 : 2 : 1.5 : 1 : 0.2, unless otherwise stated. When particular subunits were not used, the volume was made up with Tris-EDTA (TE, 10 mM Tris, 1 mM EDTA pH7), or blank vector, or the volume of transfection reagent was reduced, with equivalent results. In some experiments cDNA for the non-conducting potassium channel Kir2.1-AAA (Tinker et al., 1996) was used as control for the presence of γ_7, also with equivalent results to the use of blank vector.

PC12 cells were grown in D-MEM, 7.5% FBS and 7.5% horse serum. For electrophysiology, PC12 cells were transiently transfected with cDNAs for GFP and/or γ_7, using Fugene6. Differentiation was with serum-free medium containing NGF (100 $ng.ml^{-1}$ murine 7s NGF, Invitrogen, Paisley, UK), replenished every 48 h. Cells were used for recording after 5 -7 days of differentiation. For the generation of stable cell lines, PC12 cells were transfected with γ_7-HA or γ_7-CFP and clonal cell lines were established by standard techniques, using 400 $\mu g.ml^{-1}$ Geneticin (Invitrogen) for selection. The culture medium was subsequently supplemented with 400 μg/ml Geneticin (Invitrogen).

To obtain high transfection rates with shRNAs, PC12 cells were transfected using an Amaxa Nucleofector, according to manufacturer instructions (Amaxa, Cologne, Germany). The

DNA mix contained 2 μg of shRNA plasmid and 0.5 μg of GFP or YFP as a reporter of transfected cells. Cells were used 4 to 5 days after transfection with shRNA.

For primary culture of superior cervical ganglion (SCG) neurons, rats were killed by either CO_2 inhalation or cervical dislocation, according to UK Home Office Schedule 1 Guidelines. SCGs were dissected from rats at postnatal day 17. Ganglia were desheathed and lightly gashed before successive collagenase (Sigma) and trypsin (Sigma) treatment, both at 3 mg/ml. To produce a single-cell suspension, ganglia were dissociated by trituration and centrifugation. Dissociated cells were plated onto glass-bottomed plates (MatTeK Corp., Ashland, USA) pre-coated with laminin (Sigma), using 1 ganglion per 5 plates. Cells were maintained with Liebovitz L-15 medium (Sigma), supplemented with 24mM $NaHCO_3$, 10% FBS (Gibco), 33mM glucose (Sigma), 20mM L-glutamine, 1000 IU Penicillin, 1000 IU Streptomycin (Gibco) and 50ng/ml NGF.

Microinjection

cDNAs were injected into SCG neurons 18-24h after they were placed in culture. Microinjection was performed using an Eppendorf microinjection system on a Zeiss Axiovert 200M microscope using the following settings: 100-150 hPa injection pressure, an injection time of 0.2 s and constant pressure of between 40-50 hPa. The cDNAs were injected at 50ng/μl diluted in 200mM KCl.

Measurement of mRNA levels by q-PCR

RNA was isolated using RNeasy columns (Qiagen), including an on-column DNase step. Reverse transcription was carried out using random hexamer primers and Moloney Murine Leukemia Virus Reverse Transcriptase (Promega, Southampton, UK) at 37°C for 2 h. The q-PCR was performed with an iCycler (BioRad, Hercules CA, USA) using the iQ SYBR supermix. For each set of primers and for every experiment a standard curve was generated using a serial dilution of reverse-transcribed RNA combined from several samples. For q-PCR in PC12 cells, the following primers were used: rat $Ca_V2.2$ (NM147141) 5′-GGCAAGAAGGAGGCAGAG-3′, 5′-GCAGAAGCGACGGAGTAG-3′; rat γ_7 (AF361345) 5′-CTACTCGGGCCAGTTTCTGC-3′, 5′-GCCGGAGGGTAATTTTGC-3′; and rat glyceraldehyde-3-phosphate dehydrogenase GAPDH (AF106860) 5′-ATGACTCTACCCACGGCAAG-3′, 5′-CAT ACT CTG CAC CAG CAT CTC-3′; Data were normalized for expression of GAPDH mRNA.

For measurement of mRNA degradation rates, q-PCR of transcript levels was performed in *Xenopus* oocytes. Plasmid cDNAs were injected intranuclearly for $Ca_V2.2$, β1b, α2δ-2, either with or without γ_7. After 24 h, oocytes were incubated for the stated times with actinomycin D (50 μg/ml). RNA extraction, RT and q-PCR were performed as described above. The following primers were used: $Ca_V2.2$: 5′-CTCTGCGCTTACTGAGAATC-3′ and 5′-AACAGGAAGAGCAGGAAGAG-3′; 18S: 5′-TGACTCAACACGGGAAACCT-3′ and 5′-AATCGCTCCACCAACTAAGAAC-3′; α2δ2: 5′-GGTATTTGCTGCCACTGATG-3′ and 5′-AGGCTGCGACGGTAGAAG-3′; KCC1: 5′-AGCATAAGGTTTGGAAGAAGTG-3′ and 5′-CAGGCGGAGGTGATACAG-3′. Data were normalized for expression of 18S ribosomal RNA.

Oligoribonucleotide binding to hnRNP A2

This was performed as described previously (Hoek et al., 1998), with the exception that mouse brain, rather than rat brain, was used as a source of hnRNP A2. The following RNA oligonucleotides were used A2RE 5′-Biotin: GCCAAGGAGCCAGAGAGCAUG-3′; $Ca_V2.2$ 5′-Biotin: GCCAAGGAGCGGGAGCGAGUC-3′; Non-specific 5′-Biotin:

CAAGCACCGAACCCGCAACUG-3′. A2RE and non-specific sequences are identical in base composition (Hoek et al., 1998). Proteins were taken up in 200 μl of SDS sample buffer and heated at 65° C for 10 minutes. 20 μl of each was run on a 4-12% Bis-Tris gel and western blotting and immunodetection was performed with anti-hnRNP A2 Ab (Autogen Bioclear, 1:200).

Yeast two hybrid assay

Assays were carried out using the MATCHMAKER GAL4 two hybrid system (Clontech). Fragments of hnRNP A2 (amino acids 1-177 or 178-342), the γ7 C-terminus (201-275), the $Ca_V2.2$ I-II loop (360-483) and $Ca_V\beta1b$ were generated by PCR and subcloned in-frame into the vectors pACT2 and pAS2-1. Plasmids were cotransformed into the yeast strain Y190 and transformants were selected by plating onto minimal selective dropout (SD) *-Leu, -Trp* agar. Protein interactions were identified by restreaking colonies onto SD *-Leu, -Trp, -His* plates and carrying out colony-lift β-galactosidase assays, or growth assays in the presence of 10 mM 3-amino-1,2,4-triazole, according to the supplied protocol.

Immunoprecipitation

γ_7-HA was immunoprecipitated from stably transfected PC12 and transiently transfected tsA 201 cells. Endogenous γ_7 and hnRNP A2 proteins were immunoprecipitated from untransfected PC12 cells. The following general method was used. Cells were washed with ice cold phosphate buffered saline (PBS; Sigma-Aldrich, Gillingham, UK) and harvested in PBS with 10 mM EDTA and protease inhibitor cocktail (Roche Diagnostics). Cells were lysed and protein solubilized by agitation with extraction buffer (1% Igepal, 20 mM Tris, 150 mM NaCl, 1 mM EDTA, 0.5% sodium deoxycholate, 0.1% SDS and protease inhibitor cocktail, pH 7.4) for 30 min. at 4°C. Insoluble material was removed by centrifugation at 40,000 × g for 1 h at 4°C. The supernatant was cleared with 50 μg of Protein G linked to agarose beads (Sigma) for 2 h at 4°C. The supernatant was incubated with 2μg of high affinity Anti-HA Ab (Clone 3F10, Roche Diagnostics), or γ_7 C-terminus Ab, or hnRNP A2 monoclonal Ab EF67 (Santa Cruz Biotechnology, Santa Cruz, CA), overnight at 4°C with constant agitation. A further 20 μg of Protein G linked to agarose beads was added and incubated for 2 h at 4°C with constant agitation. Beads were washed twice with a high detergent buffer (1% Igepal, 20 mM Tris, 150 mM NaCl, 1 mM EDTA, protease inhibitor cocktail, pH 7.4), twice with a high salt buffer (0.1% Igepal, 20 mM Tris, 500 mM NaCl, 1 mM EDTA, protease inhibitor cocktail, pH 7.4) and twice with a low salt buffer (0.1% Igepal, 20 mM Tris, 1 mM EDTA, protease inhibitor cocktail, pH 7.4). Bound protein was removed from the beads by the addition of lauryl dodecyl sulphate (LDS) sample buffer with reducing agent (Invitrogen), and heating to 65 °C for 10 min. Samples containing immunoprecipitated endogenous γ_7 were treated with LDS buffer as above and eluted proteins concentrated by precipitation with ice-cold acetone prior to resuspension in fresh LDS buffer for polyacrylamide gel electrophoresis.

For protein sequencing, samples were separated on 4-12% Bis-Tris gels (Invitrogen) and stained with Coomassie (Simply safe Blue stain, Invitrogen). Bands of interest were excised from the gel and protein identification was performed by the Imperial College Proteomics Facility by tryptic mass fingerprinting, confirmed by MS-MS. The controls were from non-transfected cells, treated identically.

Coimmunoprecipitation of RNAs associated with hnRNP A2

PC12 cells were lysed and protein solubilized by agitation with extraction buffer containing 1% Igepal, 20 mM Tris, 150 mM NaCl, 1 mM EDTA, 0.5% sodium deoxycholate, protease inhibitor cocktail (pH 7.4), supplemented with 5U/ml RNAguard (GE Healthcare), for 30 minutes at 4°C. Samples were centrifuged (50,000 × g, 1 h at 4°C) and the corresponding

supernatant was then precleared with 50 μg protein G-sepharose. The supernatant was divided into two and either incubated with 2μg/ml of high affinity anti-HA Ab or an equivalent volume of PBS overnight at 4°C with constant agitation. A further 20 μg of protein G-sepharose was added and incubated for 2 h at 4°C with constant agitation. Beads were washed six times by centrifugation as described in the previous section, except that the wash buffers were supplemented with 5U/ml RNAguard. A small aliquot of beads was removed for protein analysis. The RNA on the remaining beads was extracted with Trizol (Invitrogen). Total RNA was reverse-transcribed with SuperScript III (Invitrogen) using random primers. PCR was performed using the primers described above.

Western blotting

Cells were processed for SDS PAGE as previously described (Raghib et al., 2001). For detection of endogenous γ_7 in PC12 cells, cells were lysed on ice by sonication for 3 × 10s, and centrifuged at 3000 × g for 3 min. This supernatant was decanted and centrifuged at 50,000 × g for 4 h at 4°C. The high-speed supernatant and membrane-containing pellet were then taken up in SDS buffer. Samples (50 μg cell lysate protein/lane) or IP samples prepared as above were separated using Novex 4-12% Tris-glycine or 4-12% Bis-Tris NuPAGE gels (Invitrogen) and transferred electrophoretically to polyvinylidene fluoride membranes. The membranes were blocked with 3% BSA / 0.02% Tween 20 and then incubated overnight at room temperature with the relevant primary Ab: rabbit anti-hnRNP A/B Ab (H-200, Autogen Bioclear, Calne, UK or Santa Cruz Biotechnology, Santa Cruz, CA, 1:1000); anti-hnRNP A/B monoclonal Ab from(F16, Autogen Bioclear, 1:1000); anti hnRNP A2 monoclonal Ab (EF-67, 1:1000 (Nichols et al., 2000)); rabbit anti-HA Ab, (Sigma, 1:1000), affinity-purified anti- γ_7 Ab (0.4 $\mu g.ml^{-1}$) or anti-$\alpha_2\delta$-2(102-117) (1 $\mu g.ml^{-1}$) (Brodbeck et al., 2002). The γ_2, γ_3 and γ_4 Abs have been described previously (Moss et al., 2003). Detection was performed using anti-rabbit or anti-mouse secondary Ab conjugated to HRP (BioRad, 1$\mu g.ml^{-1}$), and bound Abs were detected using enhanced chemiluminescence (ECL) or ECLPlus reagents (Amersham Pharmacia Biotech (APB), Little Chalfont, UK). Chemiluminescence or fluorescence was detected using a Typhoon 9410 Variable Mode Imager (APB), set in chemiluminescence or fluorescence mode, respectively. Protein bands were quantified using Imagequant 5.2, on non-saturated images.

Immunocytochemistry

Cells were fixed and permeablized for immunocytochemistry essentially as previously described (Brice et al., 1997). The primary Abs used were affinity-purified anti- γ_7 loop or tail Ab (as stated, 0.8 $\mu g.ml^{-1}$), mouse monoclonal anti-PDI (Abcam, Cambridge, UK, 1:100). Alexa Fluor 594-phalloidin (Invitrogen) was also used. Secondary Texas red, FITC or biotin-conjugated goat anti-mouse (Molecular Probes, Eugene, Oregon) or goat anti-rabbit (Sigma) Abs were applied at 10 $\mu g.ml^{-1}$ and 5 $\mu g.ml^{-1}$ respectively. When used, Texas red- or FITC-conjugated streptavidin were applied at 3.33 $\mu g.ml^{-1}$. A Cy3- tyramide signal amplification kit (Perkin Elmer) was used to detect γ_7 in SCG neurons. In some experiments, the nuclear dye 4′,6-diamidino-2-phenylindole (DAPI, 300 nM, Molecular Probes) was also used to visualize the nucleus. Cells were mounted in Vectashield (Vector Laboratories, Burlingame, CA) to reduce photobleaching, and examined on a confocal laser scanning microscope (Leica TCS SP or Ziess LSM), using a ×40 (1.3 NA) or ×63 (1.4 NA) oil-immersion objective. Optical sections were 1.5 μm. Photomultiplier settings were kept constant in each experiment and all images were scanned sequentially. In some experiments, where stated, a conventional fluorescence microscope (Axiovert 200, Zeiss) and CCD camera was used; images were captured using Volocity software (Improvision, UK).

Image processing was performed using ImageJ (http://rsb.info.nih.gov/ij/). Co-localization analysis was performed using the co-localization plugin on images converted to 8 bit.

Fluorophores are considered as co-localized in each pixel when their respective intensities are higher than the threshold (50) of their channels and when their intensity ratio is greater than 50%.

Electrophysiology

Xenopus oocytes were prepared, injected and utilized for electrophysiology as previously described (Canti et al., 1999), with the following exceptions. Plasmid cDNAs for the different VDCC subunits α1, $\alpha_2\delta$-2, β1b and other constructs such as γ_7 were mixed in equivalent weight ratios at 1 $\mu g.\mu l^{-1}$, unless otherwise stated, and 9 nl injected intranuclearly, following appropriate dilution**.** The recording solution for $Ca_V2.2$-injected oocytes contained (in mM): $Ba(OH)_2$ 10; TEA-OH 80; CsOH 2; Hepes 5 (pH 7.4 with methanesulfonic acid).

Whole-cell patch-clamp recording using tsA 201 or PC12 cells was performed and analyzed as described (Meir et al., 2000), with 1 mM Ba^{2+} as charge carrier (unless stated) and a holding potential of -100mV. Currents were measured 10 ms after the onset of the test pulse and the average over a 2 ms period was calculated and used for analysis. Data are expressed as mean ± s.e.m and I-V plots were fit with a modified Boltzmann equation as described (Canti et al., 2001).

Results

The reduction of functional $Ca_V2.2$ protein by γ_7 is mediated via the C-terminus of γ_7

These experiments were initiated in the light of our previous finding that co-expression of γ_7 reduced $Ca_V2.2$ protein level, as well as its functional expression (Moss et al., 2002). We have now dissected the region of γ_7 responsible for the inhibitory effect by making constructs lacking most or part of the cytoplasmic C-terminus, γ_7(1-217) and γ_7(1-238) (Fig. 1*A*). Following cDNA injection in *Xenopus* oocytes, when full-length γ_7 was co-expressed with $Ca_V2.2$ it produced ~90 % suppression of $Ca_V2.2$ currents (Fig. *1B, C*). In contrast, the shorter γ_7(1-217) transmembrane construct had very little influence on the expression of $Ca_V2.2$ currents (Fig. 1*B, C*), whereas the γ_7(1-238) construct produced a partial reduction of the $Ca_V2.2$ current (Fig. 1*C*). The C-terminal motif (T/S-SPC) is conserved between γ_7 and γ_5. Although this does not represent a classical PDZ binding motif, we investigated the importance of this epitope in mediating the effects of γ_7 on $Ca_V2.2$ currents. A construct lacking these four amino acids (γ_7(1-271)) was as effective as γ_7 in reducing $Ca_V2.2$ I_{Ba} (Fig. 1*C*), indicating that this motif is not involved in the effect of γ_7. Furthermore, addition of a C-terminal tag, such as haemaglutinin (HA) or CFP, did not affect the ability of γ_7 to suppress the expression of $Ca_V2.2$ currents. For γ_7-HA, 72.5 ± 10.1 % (n=5) inhibition of $Ca_V2.2$ currents was observed. These results indicate that a region of the γ_7 C-terminus between R217 and S271 is responsible for inhibiting $Ca_V2.2$ expression.

The role of the C-terminus of γ_7 was confirmed in tsA-201 cells. Here again the truncated γ_7(1-217) produced no inhibition of $Ca_V2.2$ currents (5.1 ± 18.6 %, Fig. 1*D, E*), whereas full-length γ_7 produced 94.9 ± 18.6 % inhibition (Fig. 1*D, E*). To confirm that the γ_7 protein was responsible for this effect, we showed that a γ_7 construct containing a stop codon prior to the first transmembrane domain produced no inhibition (Fig. 1*D, E*). Furthermore, in contrast to the effect of γ_7 on $Ca_V2.2$ currents, it had no significant effect on $Ca_V3.1$ currents (Fig. 1*D, E*).

We raised two antipeptide Abs against γ_7, to unique peptides in the linker between transmembrane segments I and II, and in the C-terminus. Neither Ab recognised any protein

bands in untransfected Cos-7 cells (Fig. 2*A*), and neither Ab cross-reacted with other γ proteins tested (Supplemental Fig. 2*A*-*C*). We then confirmed that the truncated γ_7 constructs were all expressed at a similar level to full-length γ_7, and that the truncated constructs were of the expected size (Fig. 2*A*). Next, we examined the effect of γ_7 and its C-terminal truncations on the level of $Ca_V2.2$ protein. Both γ_7 and γ_7(1-271) produced approximately 70% inhibition of $Ca_V2.2$ protein, whereas γ_7(1-217) caused no reduction (Fig. 2*B*). The extent to which $Ca_V2.2$ protein expression was suppressed by γ_7 and its truncated constructs was closely correlated with the degree of inhibition of $Ca_V2.2$ I_{Ba} observed in *Xenopus* oocytes (Fig. 2*C*). As a control, we showed that expression of an unrelated protein of similar size to γ_7 ($K_V3.1b$) had no effect on $Ca_V2.2$ protein expression (Fig. 2*B*).

γ_7 markedly reduces the stability of $Ca_V2.2$ mRNA

Several mechanisms could underlie the suppression of $Ca_V2.2$ currents and $Ca_V2.2$ protein by γ_7, including suppression of channel translation, more rapid protein degradation, suppression of channel transcription or increased mRNA breakdown. We addressed this question by examining the effect of γ_7 on the level and stability of $Ca_V2.2$ mRNA. We found that co-expression of γ_7 reduced $Ca_V2.2$ mRNA levels in two expression systems examined. In Cos-7 cells there was a 64 % reduction in $Ca_V2.2$ mRNA level in the presence of γ_7, 48 h after transfection (Supplemental Fig. 3). In agreement with this, when $Ca_V2.2$ and γ_7 were co expressed in individual *Xenopus* oocytes, there was a 66 % reduction in $Ca_V2.2$ mRNA expression after 24 h (Fig. 3*A*, see time 0) when compared to control. We then examined whether this was due to an increase in the rate of degradation of $Ca_V2.2$ mRNA. The transcription inhibitor actinomycin D was applied 24 h after injection of the relevant cDNAs into *Xenopus* oocytes (at time T_0), and mRNA levels were then determined in individual oocytes at times up to 24 h thereafter. The half-life of $Ca_V2.2$ mRNA was 7.8 ± 1.5 h under control conditions (in agreement with Schorge et al. (1999)), and it showed more than a two-fold decrease to 3.5 ± 1.1 h in the presence of γ_7 (Fig. 3*A, B*). Importantly, the truncated γ_7(1-217) construct, lacking the C-terminus, had no effect on $Ca_V2.2$ mRNA degradation rate (Fig. 3*A, B*), in agreement with its lack of effect on $Ca_V2.2$ currents or $Ca_V2.2$ protein (Figs. 1 and 2).

The relative mRNA concentrations at 24 h in the absence and presence of γ_7 are in agreement with an effect only on the degradation rate of $Ca_V2.2$ mRNA, and not on its synthesis rate. Fitting the data to the equation $d[RNA]/dt = k_f - k_d*[RNA]$, where [RNA] is the concentration of RNA at time t and k_f and k_d are the dominant rate constants for RNA synthesis and degradation, respectively, then [RNA] at time $t = (k_f/k_d)(1-\exp(-k_d*t))$. From the calculated values of k_d, k_f = 10.1 %/h and 8.8 %/h in the absence and presence of γ_7, respectively, relative to the control $Ca_V2.2$ mRNA level at 24 h, immediately before actinomycin D treatment. Thus the data provides no evidence of a marked effect of γ_7 on the synthesis rate (k_f) of $Ca_V2.2$ mRNA, despite an over 2-fold increase in the measured degradation rate.

The effect of γ_7 on mRNA stability does not affect all calcium channel subunits, as the degradation rate of $\alpha_2\delta$-2 mRNA was not affected by γ_7 co-expression (half-life ~25 h, Fig. 3*B*, Supplemental Fig. *4A*). In agreement with this, the level of $\alpha_2\delta$-2 protein was little affected by γ_7 (14.9 ± 2.8 % reduction, n=6, Supplemental Fig. 4*B*).

We also investigated the effect of γ_7 on the stability of KCC1 mRNA (a potassium chloride co-transporter), since it is a membrane protein of similar mass to $Ca_V2.2$, whose mRNA has some common sequence motifs (see below). Although KCC1 mRNA was much more stable than that of $Ca_V2.2$ (half life 50.5 h), γ_7 decreased its half-life to 18.3 h, thus increasing its mRNA turnover from 28 ± 11% to 63 ± 5 % in 24 h ($n \geq 9$) (Fig. 3*B*). Using the method

described above, again we found no evidence for any effect on the synthesis rate. The k_f was calculated to be 5.0 %/h and 4.1 %/h in the absence and presence of γ_7, respectively, relative to the control KCC1 mRNA level at 24 h. These results indicate that the effect of γ_7 on mRNA degradation rate is selective for certain mRNAs, but not selective for $Ca_V\alpha 1$ mRNAs.

In addition, we demonstrated that γ_7 had the same effect on endogenous $Ca_V2.2$ mRNA, since 9 h after actinomycin D treatment, the $Ca_V2.2$ mRNA level in a PC12 cell line stably transfected with γ_7-CFP was reduced by 74 % compared to a control PC12 cell line stably transfected with pcDNA3.1 (Fig. 3*C*, insert), and the endogenous $Ca_V2.2$ mRNA turnover rate was correspondingly enhanced (Fig. 3*C*). The half-life of $Ca_V2.2$ mRNA was 19.5 h in the pcDNA3.1 transfected PC12 cell line, which was not significantly different from that in control PC12 cells (16.9 h, data not shown). In γ_7-transfected PC12 cells the half-life was 9.1 h (Fig. 3*C*).

We found no evidence that the effect of γ_7 involves the induction of endoplasmic reticulum (ER) stress or the unfolded protein response, although this has been postulated as a mechanism of action of TARP γ_2 (Sandoval et al., 2007). Co-expression of $Ca_V2.2$ with γ_7 in tsA 201 cells, at a high transfection efficiency using Amaxa nucleofection, did not increase the editing of X binding protein (XBP) or induce C/EBP homologous protein (CHOP) expression, both of which are markers of the induction of the unfolded protein response (Harding et al., 2002), whereas these responses were evoked by exposure of cells to tunicamycin or dithiothreitol, both of which are well-known activators of ER stress (DJC and ACD, unpublished results).

Knockdown of γ_7 increases endogenous $Ca_V2.2$ mRNA level in PC12 cells

To study the physiological role of endogenous γ_7, we chose to silence its expression using RNA interference. We first examined the presence and localization of native γ_7 in PC12 cells. Immunocytochemical localization showed that endogenous γ_7 is expressed in these cells (Fig. 4*A* and Supplemental Fig. 5). We therefore used this cell line to examine the effect of knock-down of γ_7. We designed three shRNAs specifically complementary to sequences in either rat or human γ_7 mRNA. To confirm the effectiveness of the γ_7 shRNAs, we made a PC12 cell line over-expressing human γ_7-CFP, and showed that 5 days after transfection, a mix of three shRNAs directed against human γ_7 mRNA reduced the γ_7-CFP protein level in this cell line, by 75% compared to control transfected cells (Fig. 4*B, C*). We also found the three corresponding rat γ_7 shRNAs reduced endogenous γ_7 mRNA levels in PC12 cells, either individually or when mixed, whereas the control Drosophila *gnu* shRNA did not (Fig. 4*D*). This would represent a larger reduction in individual transfected cells, taking into account the incomplete transfection efficiency (about 30 %). Furthermore, the native γ_7 protein present endogenously in PC12 cells (Fig. 4*A, E*) was depleted by 70 ± 6 % in individual PC12 cells, following transfection with the rat γ_7 shRNAs (Fig. 4*E, F*).

If γ_7 is playing a physiological role in controlling mRNA stability, its knockdown might be expected to have an effect opposite to γ_7 over-expression, to increase the endogenous $Ca_V2.2$ mRNA level and enhance its stability. This was indeed the case, as $Ca_V2.2$ mRNA levels were increased by about 30 % following rat γ_7 shRNA transfection (Fig. 5*A*), which would represent a larger enhancement in individual transfected cells, taking into account the transfection efficiency. An expected physiological correlate of this would be an increase in calcium channel currents in differentiated PC12 cells. In agreement with this, we recorded a 33.1 ± 4.1% (n = 48) increase in peak somatic calcium channel current density in PC12 cells transfected with rat γ_7 shRNAs over the same time scale (Fig. 5*B*).

γ_7 exists in a complex with RNA binding proteins

Since PC12 cells contain endogenous γ_7, they represent a suitable model cell type in which to search for protein complexes containing γ_7. For this study we used a PC12 cell line stably expressing γ_7 with a C-terminal HA tag. Following immunoprecipitation of γ_7-HA from the γ_7-HA PC12 cell line, and extensive washing, the presence of co-immunoprecipitating proteins, representing proteins in a complex with γ_7, was examined by SDS-PAGE (Fig. 6*A*). Bands of interest, which were present in the γ_7-HA immunoprecipitate, but absent from the control, non-transfected PC12 cells (Fig. 6*A*, left, arrows, representative of 3 experiments), were excised and identified, following tryptic digestion, by peptide mass fingerprinting. The bands labeled (1, 36 kDa) and (2, 37 kDa) were both identified, with 34 and 38 % peptide coverage, respectively, to be heterogeneous ribonuclear protein A2 (hnRNP A2), which has a number of splice variants of 33 - 38 kDa (Hatfield et al., 2002). Band 2 also contained hnRNP A3 (40 % coverage), which shares extensive sequence homology and is found in a complex with hnRNP A2 (Ma et al., 2002). The presence of γ_7-HA was confirmed by immunoblotting (Fig. 6*A*, right). Both hnRNP A2 and hnRNP A3 are members of the hnRNP A/B sub-family.

We then confirmed that immunoprecipitation of γ_7-HA was able to pull-down endogenous hnRNP A/B proteins in another system, tsA-201 cells transiently transfected with γ_7-HA (Fig. 6*B*). Three bands were detected (36 - 42 kDa), using hnRNP A/B Abs, which, according to the antibody specificity and molecular weights are likely to represent one or more of hnRNP A1, A2 and A3, all of which also have splice variants. No hnRNP A/B immunoreactivity was immunoprecipitated by γ_7(1-217)-HA, under the same conditions (Fig. 6*B*), indicating that these hnRNPs utilize the C-terminus of γ_7 for this interaction. This is in agreement with our previous finding that the C-terminus of γ_7 is essential for its functional effects. No hnRNP A/B immunoreactive proteins were co-immunoprecipitated with an unrelated HA-tagged protein, HA-$Ca_V\beta1b$ (Fig. 6*C*), indicating that the HA tag is not responsible for this binding.

We also found that pull-down of endogenous γ_7 from untransfected PC12 cells, with the γ_7 C-terminal Ab was able to immunoprecipitate endogenous hnRNP A2 (Fig. 6*D*).

The C-terminus of hnRNP A2 interacts directly with the C terminus of γ_7

To determine whether the interaction between γ_7 and hnRNP A2 was direct, we employed the yeast two-hybrid technique. When the γ_7 C-terminus (residues 201-275) was used as bait, we found an interaction with the C-terminus of hnRNP A2 (residues 178-342, Fig. 6*E*, lane 2). Because of our previous work in this area, we used the high affinity (~10 nM, Leroy et al., 2005) interaction between the I-II linker of $Ca_V2.2$ and the $Ca_V\beta1b$ subunit as a positive control (Fig. 6*E*, lane 1). According to the relative time taken for colonies to turn blue in a colony-lift filter assay, the interaction between hnRNP A2 and γ_7 C-terminus is weaker than that between $Ca_V2.2$ and $Ca_V\beta1b$ (data not shown). As negative controls, we showed that there was no interaction between the C-termini of either hnRNP A2 or γ_7 and $Ca_V\beta1b$ (Fig. 6*E*, lanes 3 and 4). Furthermore, the N-terminus of hnRNP A2 (amino acids 1-86) was found not to interact with the C-terminus of γ7 (data not shown). All these data indicate that γ_7 is likely to be present in a complex with hnRNP A2. Nevertheless, we cannot rule out that hnRNP A3, which shows marked homology to hnRNP A2, also interacts with γ_7, either directly or by binding to hnRNP A2.

hnRNP A2 co-localizes with γ_7 in neuronal cytoplasm

We used immunocytochemistry to examine whether γ_7 and hnRNP A2 are co-localized in SCG neurons. Although, as expected, most hnRNP A2 is localized in the nucleus, it is also observed in small cytoplasmic granules in SCG neurons (Fig. 6*F*, i). In the somatic

cytoplasm there are clear regions of co-localization of both transfected γ_7-CFP and endogenous γ_7 with hnRNP A2 (Fig. 6*F* ii and iii). This is in agreement with our suggestion that γ_7 may sequester free hnRNP A2, as outlined in Fig. 9*A, B*.

$Ca_V2.2$ mRNA binds to hnRNP A2

The hnRNP A2 proteins are highly expressed in brain, and are primarily present in the nucleus, where they bind to particular nucleotide sequences in mRNA. The combination of mRNA with its many bound proteins, including hnRNP A2, then exits the nucleus as ribonucleoprotein particles (Pinol-Roma, 1997). The interaction with hnRNP A2 has been found to stabilize certain mRNAs for trafficking to a remote site of protein synthesis (Hoek *et al.*, 1998), and also to enhance translation (Kwon et al., 1999). In neurons and oligodendrocytes, hnRNP A2 has been implicated in the transport of mRNAs containing an A2 response element (A2RE) sequence, for local protein synthesis (Hoek et al., 1998; Shyu and Wilkinson, 2000).

We therefore examined whether $Ca_V2.2$ mRNA could be present in a complex with hnRNP A2. We found that the $Ca_V2.2$ mRNA used in this study contains at least two highly conserved sequences predicted to bind hnRNP A2 (Table 1), from the consensus sequence identified in MBP mRNA (Ainger et al., 1997). These two sequences are in constitutive exons, present in all splice variants of $Ca_V2.2$. The sequences preserve A and G at positions 8 and 9, previously shown to be essential for hnRNP A2 binding and function (Ainger et al., 1997; Shan et al., 2003), and the sequences are highly conserved in $Ca_V2.2$ between species (Table 1), with related sequences being found in $Ca_V2.1$ (data not shown). We found that a biotinylated 21 base ribonucleotide corresponding to sequence 1 from $Ca_V2.2$ (Table 1) binds endogenous hnRNP A2 from a mouse brain lysate, to a similar extent to the sequence originally described from MBP (Hoek et al., 1998) (Fig. 7*A*). We further found that an anti-HA Ab co-immunoprecipitated N-terminally HA-tagged hnRNP A2, both with over-expressed full-length rabbit $Ca_V2.2$ mRNA in tsA 201 cells (data not shown), and also with endogenous $Ca_V2.2$ mRNA in PC12 cells (Fig. 7*B*). Furthermore an anti-hnRNP A2 monoclonal Ab co-immunoprecipitated endogenous hnRNP A2 together with endogenous $Ca_V2.2$ mRNA from PC12 cells (Fig. 7*C*).

hnRNP A2 enhances the expression of $Ca_V2.2$ currents, and this is counteracted by γ_7

Since hnRNP A2 binds to $Ca_V2.2$ mRNA, we wished to examine the consequences on calcium channel expression of co-expression with hnRNP A2. When this construct was co-expressed with $Ca_V2.2/\beta1b/\alpha_2\delta$-2 in *Xenopus* oocytes, it produced a significant enhancement of the peak calcium current amplitude, without affecting the current kinetics or voltage-dependence (Fig. 7*D*). In experiments performed in parallel, an unrelated hnRNP (A1), that is involved in mRNA processing and export but does not bind to A2RE sequences (Cullen, 2000), did not enhance $Ca_V2.2$ calcium currents (Fig. 7D). Thus hnRNP A2 may enhance $Ca_V2.2$ mRNA stability in *Xenopus* oocytes or increase its transport to sites of translation. This is compatible with the role previously attributed to hnRNP A2, that it enhances both transport and translation of specific mRNAs (Kwon et al., 1999). We also found that the effect of hnRNP A2 was able to generalize to other Ca_V2 channels, as enhancement of $Ca_V2.1/\beta4/\alpha_2\delta$-2 currents was also observed, the peak I_{Ba} at +5 mV being increased to 194.8 ± 19.9 % of control (n = 28, $P = 0.0004$). $Ca_V2.1$ mRNA contains A2RE sequences that are homologous to those of $Ca_V2.2$ (data not shown).

We then investigated whether there was an interaction between the effects of hnRNP A2 and γ_7 on calcium channel current expression. The inhibitory effect of γ_7 on $Ca_V2.2$ calcium channel currents, shown in Fig. 1*B*, was found to be concentration-dependent (data not shown), and a low concentration of γ_7 was chosen (1:4 dilution of γ_7 cDNA), that did not

inhibit $Ca_V2.2$ currents in the *Xenopus* oocyte expression system (Fig. 7*E*), in order to examine its interaction with the effect of hnRNP A2. We found that the enhancement of $Ca_V2.2$ currents by hnRNP A2 was prevented by co-expression of this low concentration of γ_7 (Fig. 7*E*). This indicates that γ_7 opposes the effect of hnRNP A2, supporting the hypothesis that the binding of hnRNP A2 to its binding site on the C-terminus of γ_7 reduces the amount available to interact with $Ca_V2.2$ mRNA in the cytosol. In agreement with this interpretation, expression of the cytosolic C-terminus of γ_7 (γ_7 (201-275)), which our yeast two hybrid data shows to be able to bind hnRNP A2 (Fig. 6*E*), was itself able to reduce the amplitude of $Ca_V2.2$ currents. In experiments similar to those shown in Fig. 1*B*, the peak $Ca_V2.2$ I_{Ba} current amplitude was reduced by 70 .6 ± 4.5 % (n = 19) relative to control currents, in the presence of the C-terminus of γ_7 (data not shown), compared to an 87.4 % reduction by full-length γ_7 in the same experiment.

Investigation of the subcellular localization of γ_7

The topology of γ_1 and the TARP γ proteins indicates that the linker between the first and second transmembrane domains is extracellular (Chu et al., 2001) and the same might be anticipated for γ_7, which has a predicted glycosylation site in this loop (see Fig. 1*A*). We obtained mutational evidence that γ_7 is N-glycosylated on N45 in the I-II loop, supporting the proposed topology (Fig. 8*A*). However, heterologously expressed γ_7 is not inserted in the plasma membrane of tsA 201 cells, since it was not detected with an Ab to this I-II loop in non-permeabilized cells (Fig. 8*B*).

We have observed that γ_7-CFP, when heterologously expressed in cultured SCG neurons, is present, in part, in motile intracellular vesicles (Fig. 8*C* and data not shown). These co-localize with γ_7 I-II loop Ab immunoreactivity only when the cells are permeabilized (Fig. 8*C*). No plasma membrane staining was detected in the absence of cell permeabilization (Fig. 8*C*). We also found that neither endogenous γ_7 (Fig. 4*A*), nor γ_7-CFP (Fig. 4*B* and data not shown) localized to the plasma membrane in PC12 cells. The localization of γ_7 is therefore on intracellular membranes in all the cells we have examined. We found that the distribution of γ_7-CFP partially overlapped with that of an ER marker in the somata of SCG neurons microinjected with γ_7-CFP and pDsRed2-ER (Fig. 8*D*). It was also found in vesicular structures, which were negative for the ER marker (Fig. 8*D*). Similar results were obtained in PC12 cells using a different ER marker, protein disulfide isomerase (data not shown).

Discussion

We have previously described the identification of two genes that encode γ_5 and γ_7, by their homology with the mouse *stargazin* gene (*cacng2*), and have cloned and expressed the cDNA for both human and mouse γ_7 (Moss et al., 2002). The γ_7 protein contains 275 amino acids with an estimated protein mass of 31 kDa, and has four predicted transmembrane-spanning domains with intracellular N- and C-termini and a consensus N-glycosylation sequence in the loop between the first two transmembrane segments (Fig. 1*A*). Together with the other γ-like proteins, it belongs to the claudin super-family, members of which play diverse roles in cellular physiology (Sanders et al., 2001). Initially the novel γ_1-like proteins ($\gamma_{2\text{-}8}$) were investigated as potential calcium channel subunits (Letts et al., 1998; Klugbauer et al., 2000; Sharp et al., 2001; Kang et al., 2001; Rousset et al., 2001; Moss et al., 2003). However, we have shown that while the human γ_2 and γ_4 TARPS are expressed in Purkinje neurons, there was no effect of these proteins on calcium currents composed of $Ca_V2.1/\beta4/\alpha_2\delta$-2, a combination which mimics the major calcium channel complement in Purkinje cells (Moss et al., 2003). More recently these proteins have been shown to have roles in trafficking and localization of AMPA glutamate receptors (Tomita et al., 2003; Tomita et al., 2004; Fukata et al., 2005; Kato et al., 2007). Together with the data presented here, these

findings suggest that γ-proteins may play diverse and possibly multiple roles in intracellular trafficking.

In our original study, we showed that co-expression with γ_7 almost completely abolished Ba^{2+} current through N-type $Ca_V2.2$ channels expressed from cDNA in both *Xenopus* oocyte and Cos-7 cell expression systems (Moss et al., 2002). Several mechanisms could underlie the suppression of $Ca_V2.2$ currents by γ_7 protein, but we have now identified that a major mechanism of suppression of $Ca_V2.2$ currents by γ_7 results from a decrease in $Ca_V2.2$ mRNA stability. This process requires the cytoplasmic C-terminus of γ_7, since all its effects, to inhibit $Ca_V2.2$ current and protein expression and to increase the rate of mRNA degradation, are completely prevented by the removal of most of the C-terminus of γ_7. It is well known that the effect of over-expression of a protein does not necessarily reflect its physiological function, since an over-expressed protein may act to sequester interacting partners. However, our evidence indicates that the regulation of the stability of $Ca_V2.2$ mRNA, and potentially other mRNAs, represents an important role for native γ_7. This evidence stems from the finding that knockdown of endogenous γ_7 in PC12 cells, using γ_7 shRNA, substantially enhances their endogenous $Ca_V2.2$ mRNA level and enhances endogenous somatic calcium currents following differentiation.

We have subsequently identified by co-immunoprecipitation from a PC12 cell line stably transfected with γ_7-HA, that the RNA binding protein hnRNP A2 is co-immunoprecipitated with γ_7. hnRNP A2 has been found to be involved in the stability, trafficking and localization of particular mRNAs and has been identified to bind to several different mRNA sequences including CGG repeats (Sofola et al., 2007), AU-rich elements (Hamilton et al., 1999), and a well-characterized binding motif termed A2RE (Ainger et al., 1997; Shan et al., 2003; Fahling et al., 2006). Most hnRNP A2 is localized in the nucleus, where it binds to specific sequences in transcribed mRNA, and is involved in mRNA export into the cytoplasm (for review see Shyu and Wilkinson, 2000), and subsequently in trafficking and enhancement of translation for those mRNAs containing an A2RE sequence (Kwon et al., 1999). Our yeast two-hybrid data indicates that γ_7 C-terminus binds directly to hnRNP A2, and our subcellular localization data for γ_7 indicates that this interaction will occur on intracellular membranes within the cytoplasm (as depicted in Fig. 9*B*).

There are two highly conserved consensus hnRNP A2-binding A2RE motifs in the $Ca_V2.2$ mRNA used in this study (Table 1), that contain the conserved A and G at positions 8 and 9, which have been found to be a prerequisite for binding of hnRNP A2 (Ainger et al., 1997). There are also several other, less well-conserved, A2RE motifs in the $Ca_V2.2$ mRNA sequence, that may also be functional (data not shown). Here we have demonstrated that hnRNP A2 binds to one of the conserved sequences (Table 1, sequence 2), and by homology is highly likely to bind to the other sequence. Furthermore hnRNP A2 co-immunoprecipitates endogenous $Ca_V2.2$ mRNA from PC12 cells. We suggest that hnRNP A2 normally binds to sequences on $Ca_V2.2$ mRNA in the nucleus and when the ribonucleoprotein particle so formed exits the nucleus, it is transported to its site of translation, and also protected from degradation (as depicted in Fig. 9*A*). A similar mechanism of interaction with hnRNP A2 has been proposed for MBP mRNA which contains a canonical A2RE sequence (Hoek et al., 1998). It has also been shown that hnRNP A2 itself is subject to transport (Brumwell et al., 2002). Indeed, the hnRNP-A/B proteins have been identified as components in isolated RNA-transporting granules (Kanai et al., 2004). Furthermore, the Drosophila homolog Hrp48 is involved in the localization of oskar mRNA (Yano et al., 2004; Huynh et al., 2004). Other RNA binding proteins, such as Staufen have been shown to have an effect on both localization and decay of specific mRNAs (Broadus et al., 1998; Kim et al., 2005).

Our results provoke the hypothesis that γ_7 is involved in the regulation of hnRNP A2 function, as depicted in Fig. 9*B*. γ_7 may sequester hnRNP A2, and this may be the mechanism whereby the stability of specific mRNAs, including that of $Ca_V2.2$, are compromised. Furthermore, our results indicate that native, as well as heterologously expressed γ_7 both influence the physiological regulation of $Ca_V2.2$ mRNA stability, since knock-down of native γ_7 increased endogenous $Ca_V2.2$ mRNA and $Ca_V2.2$ current levels. This indicates that endogenous γ_7 may function to limit the availability of cytoplasmic hnRNP A2. A related pathological mechanism of hnRNP A2 sequestration by binding to expanded CGG repeats of FMR1 mRNA has recently been proposed to occur in Fragile X-associated tremor/ataxia syndrome (Sofola et al., 2007). It will be of interest to examine whether a similar interaction occurs with other triplet repeat diseases.

The expression of $Ca_V2.2$ channel proteins may be particularly vulnerable to a reduction in available hnRNP A2 because the mRNA degradation rate of $Ca_V2.2$ is relatively high. Nevertheless, other mRNAs are also likely to be similarly affected, and we show that the degradation of KCC1 mRNA, which also contains an A2RE sequence, is also enhanced by γ_7.

Both $Ca_V2.2$ (Mori et al., 1991) and γ_7 (Moss et al., 2002) are selectively expressed in neurons. $Ca_V2.2$ channel expression and function is dynamically regulated both physiologically (Pravettoni et al., 2000; Inchauspe et al., 2004), and in pathology (Hendriksen et al., 1997). It is of interest that $Ca_V2.2$ channels are functionally most important in early development, and in many instances their role is later substituted by P/Q type calcium channels ($Ca_V2.1$), both in terms of somatic currents (Salgado et al., 2005) and in terms of synaptic transmission (Iwasaki et al., 2000). Over a similar time period we have found that γ_7 expression is strongly up-regulated (M. Nieto-Rostro and ACD, unpublished results). It is now recognized from many studies that regulation of mRNA stability is a very important part of the post-transcriptional control of expression of numerous genes (Wilusz and Wilusz, 2004).

There are indications that $Ca_V2.2$ mRNA is subject to transport, as it has been identified in dendritic growth cones (Crino and Eberwine, 1996) and in processes of motor neurons (Jablonka et al., 2007). Furthermore, N-type calcium channels are localized in the presynaptic terminals of peripheral neurons, such as DRG neurons, and local synthesis of transmembrane proteins has recently been demonstrated in axons and axonal growth cones (Brittis et al., 2002). It will be of great interest in the future to examine whether hnRNP A2 affects the transport of Ca_V2 family mRNAs, to regions distinct from the cell soma.

Supplementary Material

Refer to Web version on PubMed Central for supplementary material.

Acknowledgments

We thank the Wellcome Trust, BBSRC and MRC for support. LF held a fellowship from Fondation pour la Recherche Medicale and J.L. held a Wellcome Trust International fellowship. DJC was supported by a BBSRC PhD studentship and DW by a British Heart Foundation PhD studentship. We are grateful to Dr. WJ Frith for mathematical advice, Kanchan Chaggar for technical assistance, Dr. R Nichols for the hnRNP A2 constructs, Dr J Caceres for hnRNPA1 cDNA, Dr. S Alper for KCC1 cDNA, Dr. TJ Shafer for PC12 cells and Drs. A Cahill and A. Fox for pG418-shRNA-Empty vector.

References

Ainger K, Avossa D, Diana AS, Barry C, Barbarese E, Carson JH. Transport and localization elements in myelin basic protein mRNA. J Cell Biol. 1997; 138:1077–1087. [PubMed: 9281585]

Black JL, Lennon VA. Identification and cloning of putative human neuronal voltage-gated calcium channel gamma-2 and gamma-3 subunits: Neurologic implications. Mayo Clin Proc. 1999; 74:357–361. [PubMed: 10221464]

Brice NL, Berrow NS, Campbell V, Page KM, Brickley K, Tedder I, Dolphin AC. Importance of the different β subunits in the membrane expression of the α1A and α2 calcium channel subunits: studies using a depolarisation-sensitive α1A antibody. Eur J Neurosci. 1997; 9:749–759. [PubMed: 9153581]

Brittis PA, Lu Q, Flanagan JG. Axonal protein synthesis provides a mechanism for localized regulation at an intermediate target. Cell. 2002; 110:223–235. [PubMed: 12150930]

Broadus J, Fuerstenberg S, Doe CQ. Staufen-dependent localization of prospero mRNA contributes to neuroblast daughter-cell fate. Nature. 1998; 391:792–795. [PubMed: 9486649]

Brodbeck J, Davies A, Courtney J-M, Meir A, Balaguero N, Canti C, Moss FJ, Page KM, Pratt WS, Hunt SP, Barclay J, Rees M, Dolphin AC. The ducky mutation in *Cacna2d2* results in altered Purkinje cell morphology and is associated with the expression of a truncated *a2d*-2 protein with abnormal function. J Biol Chem. 2002; 277:7684–7693. [PubMed: 11756448]

Brummelkamp TR, Bernards R, Agami R. A system for stable expression of short interfering RNAs in mammalian cells. Science. 2002; 296:550–553. [PubMed: 11910072]

Brumwell C, Antolik C, Carson JH, Barbarese E. Intracellular trafficking of hnRNP A2 in oligodendrocytes. Exp Cell Res. 2002; 279:310–320. [PubMed: 12243756]

Burgess DL, Davis CF, Gefrides LA, Noebels JL. Identification of three novel Ca2+ channel gamma subunit genes reveals molecular diversification by tandem and chromosome duplication. Genome Research. 1999; 9:1204–1213. [PubMed: 10613843]

Burgess DL, Gefrides LA, Foreman PJ, Noebels JL. A cluster of three novel Ca2+ channel gamma subunit genes on chromosome 19q13.43: Evolution and expression profile of the gamma subunit gene family. Genomics. 2001; 71:339–350. [PubMed: 11170751]

Campbell V, Berrow N, Brickley K, Page K, Wade R, Dolphin AC. Voltage-dependent calcium channel β-subunits in combination with alpha1 subunits have a GTPase activating effect to promote hydrolysis of GTP by G $alpha_o$ in rat frontal cortex. FEBS Lett. 1995; 370:135–140. [PubMed: 7544301]

Canti C, Davies A, Berrow NS, Butcher AJ, Page KM, Dolphin AC. Evidence for two concentration-dependent processes for β subunit effects on α1B calcium channels. Biophys J. 2001; 81:1439–1451. [PubMed: 11509358]

Canti C, Page KM, Stephens GJ, Dolphin AC. Identification of residues in the N-terminus of α1B critical for inhibition of the voltage-dependent calcium channel by Gβγ. J Neurosci. 1999; 19:6855–6864. [PubMed: 10436043]

Catterall WA. Structure and regulation of voltage-gated Ca^{2+} channels. Annu Rev Cell Dev Biol. 2000; 16:521–555. [PubMed: 11031246]

Chu PJ, Robertson HM, Best PM. Calcium channel gamma subunits provide insights into the evolution of this gene family. Gene. 2001; 280:37–48. [PubMed: 11738816]

Crino PB, Eberwine J. Molecular characterization of the dendritic growth cone: regulated mRNA transport and local protein synthesis. Neuron. 1996; 17:1173–1187. [PubMed: 8982164]

Cullen BR. Connections between the processing and nuclear export of mRNA: evidence for an export license? Proc Natl Acad Sci U S A. 2000; 97:4–6. [PubMed: 10618360]

Dolphin AC. G protein modulation of voltage-gated calcium channels. Pharmacol Rev. 2003a; 55:607–627. [PubMed: 14657419]

Dolphin AC. β subunits of voltage-gated calcium channels. J Bioeng Biomemb. 2003b; 35:599–620.

Fahling M, Mrowka R, Steege A, Martinka P, Persson PB, Thiele BJ. hnRNP-A2/B1 modulate collagen prolyl 4-hydroxylase alpha (I) mRNA-stability. J Biol Chem. 2006

Freise D, Held B, Wissenbach U, Pfeifer A, Trost C, Himmerkus N, Schweig U, Freichel M, Biel M, Hofmann F, Hoth M, Flockerzi V. Absence of the gamma subunit of the skeletal muscle dihydropyridine receptor increases L-type Ca^{2+} currents and alters channel inactivation properties. J Biol Chem. 2000; 275:14476–14481. [PubMed: 10799530]

Fukata Y, Tzingounis AV, Trinidad JC, Fukata M, Burlingame AL, Nicoll RA, Bredt DS. Molecular constituents of neuronal AMPA receptors. J Cell Biol. 2005; 169:399–404. [PubMed: 15883194]

Hamilton BJ, Nichols RC, Tsukamoto H, Boado RJ, Pardridge WM, Rigby WF. hnRNP A2 and hnRNP L bind the 3′UTR of glucose transporter 1 mRNA and exist as a complex in vivo. Biochem Biophys Res Commun. 1999; 261:646–651. [PubMed: 10441480]

Harding HP, Calfon M, Urano F, Novoa I, Ron D. Transcriptional and translational control in the Mammalian unfolded protein response. Annu Rev Cell Dev Biol. 2002; 18:575–599. [PubMed: 12142265]

Hatfield JT, Rothnagel JA, Smith R. Characterization of the mouse hnRNP A2/B1/B0 gene and identification of processed pseudogenes. Gene. 2002; 295:33–42. [PubMed: 12242009]

Hendriksen H, Kamphuis W, Lopes da Silva FH. Changes in voltage-dependent calcium channel alpha1-subunit mRNA levels in the kindling model of epileptogenesis. Brain Res Mol Brain Res. 1997; 50:257–266. [PubMed: 9406942]

Hoek KS, Kidd GJ, Carson JH, Smith R. hnRNP A2 selectively binds the cytoplasmic transport sequence of myelin basic protein mRNA. Biochemistry. 1998; 37:7021–7029. [PubMed: 9578590]

Huynh JR, Munro TP, Smith-Litiere K, Lepesant JA, St Johnston D. The Drosophila hnRNPA/B homolog, Hrp48, is specifically required for a distinct step in osk mRNA localization. Dev Cell. 2004; 6:625–635. [PubMed: 15130488]

Inchauspe CG, Martini FJ, Forsythe ID, Uchitel OD. Functional compensation of P/Q by N-type channels blocks short-term plasticity at the calyx of held presynaptic terminal. J Neurosci. 2004; 24:10379–10383. [PubMed: 15548652]

Iwasaki S, Momiyama A, Uchitel OD, Takahashi T. Developmental Changes in Calcium Channel Types Mediating Central Synaptic Transmission. J Neurosci. 2000; 20:59–65. [PubMed: 10627581]

Jablonka S, Beck M, Lechner BD, Mayer C, Sendtner M. Defective Ca2+ channel clustering in axon terminals disturbs excitability in motoneurons in spinal muscular atrophy. J Cell Biol. 2007; 179:139–149. [PubMed: 17923533]

Jay SD, Sharp AH, Kahl SD, Vedvick TS, Harpold MM, Campbell KP. Structural characterization of the dihydropyridine-sensitive calcium channel α_2-subunit and the associated δ peptides. J Biol Chem. 1991; 266:3287–3293. [PubMed: 1847144]

Kanai Y, Dohmae N, Hirokawa N. Kinesin transports RNA: isolation and characterization of an RNA-transporting granule. Neuron. 2004; 43:513–525. [PubMed: 15312650]

Kang MG, Chen CC, Felix R, Letts VA, Frankel WN, Mori Y, Campbell KP. Biochemical and biophysical evidence for *gamma*$_2$ subunit association with neuronal voltage-activated Ca^{2+} channels. J Biol Chem. 2001; 276:32917–32924. [PubMed: 11441000]

Kang MG, Chen CC, Wakamori M, Hara Y, Mori Y, Campbell KP. A functional AMPA receptor-calcium channel complex in the postsynaptic membrane. Proc Natl Acad Sci U S A. 2006; 103:5561–5566. [PubMed: 16567654]

Kato AS, Zhou W, Milstein AD, Knierman MD, Siuda ER, Dotzlaf JE, Yu H, Hale JE, Nisenbaum ES, Nicoll RA, Bredt DS. New transmembrane AMPA receptor regulatory protein isoform, gamma-7, differentially regulates AMPA receptors. J Neurosci. 2007; 27:4969–4977. [PubMed: 17475805]

Kim YK, Furic L, DesGroseillers L, Maquat LE. Mammalian Staufen1 recruits Upf1 to specific mRNA 3′UTRs so as to elicit mRNA decay. Cell. 2005; 120:195–208. [PubMed: 15680326]

Klugbauer N, Dai SP, Specht V, Lacinová L, Marais E, Bohn G, Hofmann F. A family of gamma-like calcium channel subunits. FEBS Lett. 2000; 470:189–197. [PubMed: 10734232]

Kwon S, Barbarese E, Carson JH. The cis-acting RNA trafficking signal from myelin basic protein mRNA and its cognate trans-acting ligand hnRNP A2 enhance cap-dependent translation. J Cell Biol. 1999; 147:247–256. [PubMed: 10525532]

Leroy J, Richards MS, Butcher AJ, Nieto-Rostro M, Pratt WS, Davies A, Dolphin AC. Interaction via a key tryptophan in the I-II linker of N-type calcium channels is required for beta1 but not for palmitoylated beta2, implicating an additional binding site in the regulation of channel voltage-dependent properties. J Neurosci. 2005; 25:6984–6996. [PubMed: 16049174]

Letts VA, Felix R, Biddlecome GH, Arikkath J, Mahaffey CL, Valenzuela A, Bartlett FS, Mori Y, Campbell KP, Frankel WN. The mouse stargazer gene encodes a neuronal Ca^{2+} channel gamma subunit. Nature Genet. 1998; 19:340–347. [PubMed: 9697694]

Lingor P, Koeberle P, Kugler S, Bahr M. Down-regulation of apoptosis mediators by RNAi inhibits axotomy-induced retinal ganglion cell death in vivo. Brain. 2005; 128:550–558. [PubMed: 15659426]

Ma AS, Moran-Jones K, Shan J, Munro TP, Snee MJ, Hoek KS, Smith R. Heterogeneous nuclear ribonucleoprotein A3, a novel RNA trafficking response element-binding protein. J Biol Chem. 2002; 277:18010–18020. [PubMed: 11886857]

Meir A, Bell DC, Stephens GJ, Page KM, Dolphin AC. Calcium channel β subunit promotes voltage-dependent modulation of α1B by Gβγ. Biophys J. 2000; 79:731–746. [PubMed: 10920007]

Mori Y, Friedrich T, Kim M-S, Mikami A, Nakai J, Ruth P, Bosse E, Hofmann F, Flockerzi V, Furuichi T, Mikoshiba K, Imoto K, Tanabe T, Numa S. Primary structure and functional expression from complementary DNA of a brain calcium channel. Nature. 1991; 350:398–402. [PubMed: 1849233]

Moss FJ, Dolphin AC, Clare JJ. Human neuronal stargazin-like proteins, gamma2, gamma3 and gamma4; an investigation of their specific localization in human brain and their influence on CaV2.1 voltage-dependent calcium channels expressed in Xenopus oocytes. BMC Neurosci. 2003; 4:23. [PubMed: 14505496]

Moss FJ, Viard P, Davies A, Bertaso F, Page KM, Graham A, Canti C, Plumpton M, Plumpton C, Clare JJ, Dolphin AC. The novel product of a five-exon *stargazin*-related gene abolishes $Ca_V2.2$ calcium channel expression. EMBO J. 2002; 21:1514–1523. [PubMed: 11927536]

Nichols RC, Wang XW, Tang J, Hamilton BJ, High FA, Herschman HR, Rigby WF. The RGG domain in hnRNP A2 affects subcellular localization. Exp Cell Res. 2000; 256:522–532. [PubMed: 10772824]

Pinol-Roma S. HnRNP proteins and the nuclear export of mRNA. Semin Cell Dev Biol. 1997; 8:57–63. [PubMed: 15001106]

Powers PA, Liu S, Hogan K, Gregg RG. Molecular characterization of the gene encoding the gamma subunit of the human skeletal muscle 1,4-dihydropyridine-sensitive Ca^{2+} channel (CACNLG), cDNA sequence, gene structure, and chromosomal location. J Biol Chem. 1993; 268:9275–9279. [PubMed: 8387489]

Pravettoni E, Bacci A, Coco S, Forbicini P, Matteoli M, Verderio C. Different localizations and functions of L-type and N-type calcium channels during development of hippocampal neurons. Developmental Biology. 2000; 227:581–594. [PubMed: 11071776]

Raghib A, Bertaso F, Davies A, Page KM, Meir A, Bogdanov Y, Dolphin AC. Dominant-negative synthesis suppression of voltage-gated calcium channel $Ca_V2.2$ induced by truncated constructs. J Neurosci. 2001; 21:8495–8504. [PubMed: 11606638]

Rousset M, Cens T, Restituito S, Barrere C, Black JL III, McEnery MW, Charnet P. Functional roles of gamma2, gamma3 and gamma4, three new Ca2+ channel subunits, in P/Q-type Ca2+ channel expressed in Xenopus oocytes. J Physiol. 2001; 532:583–593. [PubMed: 11313431]

Salgado H, Tecuapetla F, Perez-Rosello T, Perez-Burgos A, Perez-Garci E, Galarraga E, Bargas J. A Reconfiguration of CaV2 Ca2+ Channel Current and Its Dopaminergic D2 Modulation in Developing Neostriatal Neurons. J Neurophysiol. 2005; 94:3771–3787. [PubMed: 16120665]

Sanders CR, Ismail-Beigi F, McEnery MW. Mutations of peripheral myelin protein 22 result in defective trafficking through mechanisms which may be common to diseases involving tetraspan membrane proteins. Biochemistry. 2001; 40:9453–9459. [PubMed: 11583144]

Sandoval A, Andrade A, Beedle AM, Campbell KP, Felix R. Inhibition of recombinant N-type Ca(V) channels by the gamma 2 subunit involves unfolded protein response (UPR)-dependent and UPR-independent mechanisms. J Neurosci. 2007; 27:3317–3327. [PubMed: 17376992]

Schorge S, Gupta S, Lin ZX, McEnery MW, Lipscombe D. Calcium channel activation stabilizes a neuronal calcium channel mRNA. Nat Neurosci. 1999; 2:785–790. [PubMed: 10461216]

Shan J, Munro TP, Barbarese E, Carson JH, Smith R. A molecular mechanism for mRNA trafficking in neuronal dendrites. J Neurosci. 2003; 23:8859–8866. [PubMed: 14523087]

Sharp AH, Black JL III, Dubel SJ, Sundarraj S, Shen JP, Yunker AMR, Copeland TD, McEnery MW. Biochemical and anatomical evidence for specialized voltage-dependent calcium channel gamma isoform expression in the epileptic and ataxic mouse, stargazer. Neuroscience. 2001; 105:599–617. [PubMed: 11516827]

Shyu AB, Wilkinson MF. The double lives of shuttling mRNA binding proteins. Cell. 2000; 102:135–138. [PubMed: 10943833]

Sofola OA, Jin P, Qin Y, Duan R, Liu H, de Haro M, Nelson DL, Botas J. RNA-Binding Proteins hnRNP A2/B1 and CUGBP1 Suppress Fragile X CGG Premutation Repeat-Induced Neurodegeneration in a Drosophila Model of FXTAS. Neuron. 2007; 55:565–571. [PubMed: 17698010]

Swick AG, Janicot M, Cheneval-Kastelic T, McLenithan JC, Lane DM. Promoter-cDNA-directed heterologous protein expression in Xenopus laevis oocytes. Proc Natl Acad Sci USA. 1992; 89:1812–1816. [PubMed: 1542676]

Tinker A, Jan YN, Jan LY. Regions responsble for assembly of inwardly rectifying potassium channels. Cell. 1996; 87:857–868. [PubMed: 8945513]

Tomita S, Chen L, Kawasaki Y, Petralia RS, Wenthold RJ, Nicoll RA, Bredt DS. Functional studies and distribution define a family of transmembrane AMPA receptor regulatory proteins. J Cell Biol. 2003; 161:805–816. [PubMed: 12771129]

Tomita S, Fukata M, Nicoll RA, Bredt DS. Dynamic interaction of stargazin-like TARPs with cycling AMPA receptors at synapses. Science. 2004; 303:1508–1511. [PubMed: 15001777]

Wilusz CJ, Wilusz J. Bringing the role of mRNA decay in the control of gene expression into focus. Trends Genet. 2004; 20:491–497. [PubMed: 15363903]

Xu X, Shrager P. Dependence of axon initial segment formation on Na+ channel expression. J Neurosci Res. 2005; 79:428–441. [PubMed: 15635682]

Yano T, Lopez dQ, Matsui Y, Shevchenko A, Shevchenko A, Ephrussi A. Hrp48, a Drosophila hnRNPA/B homolog, binds and regulates translation of oskar mRNA. Dev Cell. 2004; 6:637–648. [PubMed: 15130489]

Europe PMC Funders Author Manuscripts

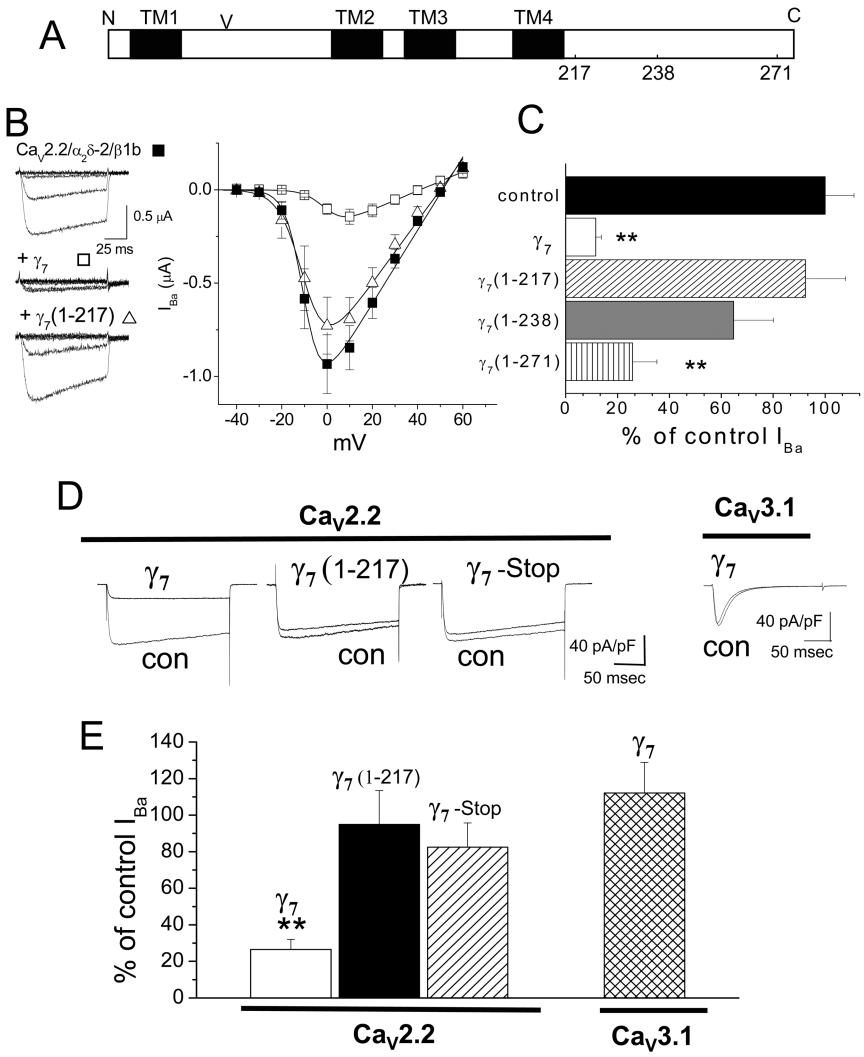

Figure 1. Effect of C-terminal truncation of γ_7 on $Ca_V2.2/\beta1b/\alpha_2\delta$-2 and $Ca_V3.1$ currents

A, Linearized diagram of γ_7, indicating the approximate positions of the 4 transmembrane (TM) segments (black bars), the N-glycosylation site (V) at N45, and the position of the truncations at amino acids 217, 238 and 271.

B, Left: example traces elicited following cDNA injection into *Xenopus* oocytes by 100 ms step depolarizations to between -40 and 0 mV from a holding potential of -100 mV for $Ca_V2.2/\beta1b/\alpha_2\delta$-2 (top), plus γ_7 (center) and plus γ_7 (1-217) (bottom). The charge carrier was 10 mM Ba^{2+}. The symbols beside the traces refer to the relevant data in the current-voltage relationship (right); $Ca_V2.2/\beta1b/\alpha_2\delta$-2 (■, n= 19), plus γ_7 (1-217) (Δ, n =18) and plus γ_7 (□, n=8). Data are fit by a modified Boltzmann function as described in Methods, with $V_{50,\,act}$ of -9.9, -9.8 and +1.2 mV respectively and G_{max} of 19.6, 16.6 and 5.9 μS, respectively.

C, Mean % of control peak I_{Ba} for $Ca_V2.2/\beta1b/\alpha_2\delta$-2 currents (black bar, n=29) when co-expressed with γ_7 (white bar, n=31) or its truncated constructs, γ_7(1-217) (hatched bar, n=15), γ_7(1-238) (grey bar, n=12) and γ_7(1-271) (striped bar, n=16). The statistical significances compared to control are ** P<0.01. There was no effect of any of the constructs on the voltage for 50 % steady-state inactivation, which from combined

Europe PMC Funders Author Manuscripts

experiments was -60.2 ± 0.8 mV for controls (n=16), -58.6 ± 1.0 mV in the presence of γ_7 (n=7), -61.7 ± 3.6 mV for γ_7(1-217) (n=5) and -59.8 ± 1.0 mV for γ_7(1-271) (n=5).

D, Representative traces of peak Ba^{2+} currents in tsA 201 cells, co-transfected with $Ca_V2.2$, β1b and $\alpha_2\delta$-2 with pMT2 as control (con), compared to γ_7 (panel 1), γ_7(1-217) (panel 2), γ_7(stop) (panel 3). Panel 4 shows $Ca_V3.1$ expression with pMT2 as control (con), compared to γ_7. Currents were elicited by depolarization to +5 mV ($Ca_V2.2$, 1 mM Ba^{2+}) or -10 mV (Ca_v 3.1, 10 mM Ba^{2+}), from a holding potential of -100 mV. Calibration bars refer to all traces for $Ca_V2.2$.

E, Mean inhibition of Ba^{2+} currents (expressed as % of control ± s.e.m.) induced by co-expression of $Ca_V2.2$ with γ_7 (white bar, n=21), γ_7 (1-217) (black bar, n=15), γ_7(stop) (hatched bar, n=28), or $Ca_V3.1$ with γ_7 (cross-hatched bar, n=29). Statistical significance compared to the current size without γ_7 ** $P<0.01$, Student's t test.

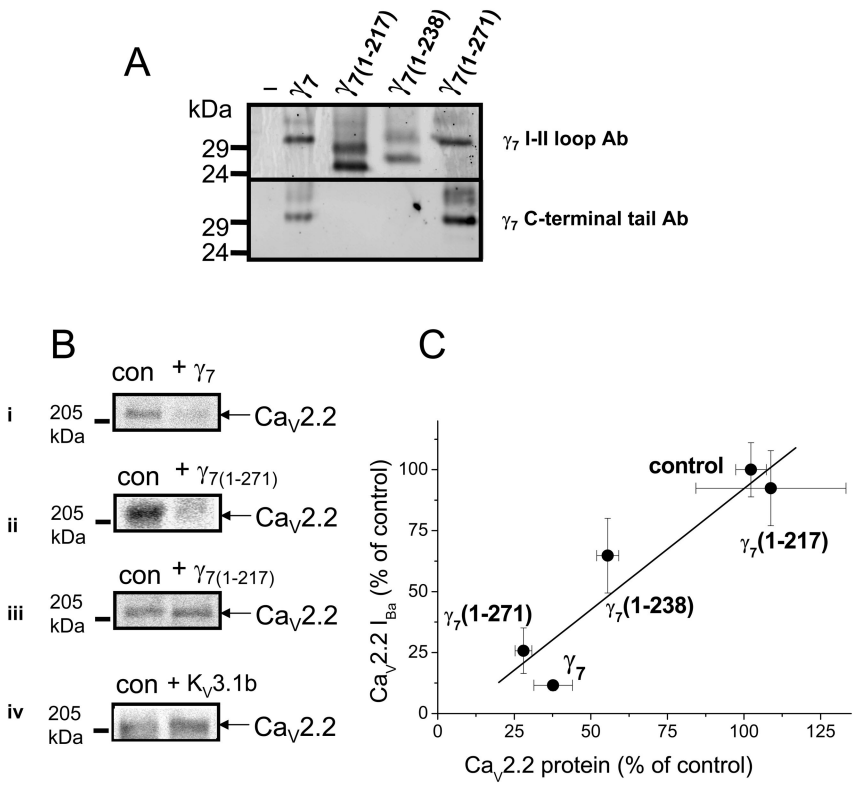

Figure 2. Effect of C-terminal truncation of γ_7 on $Ca_V2.2$ protein

A, γ_7 and truncated γ_7 constructs were expressed at the expected sizes in Cos-7 cells (upper panel γ_7 I-II loop Ab, lower panel γ_7 C terminal tail Ab). In each lane, the lower band corresponds to the expected protein molecular weight, and the upper band(s) correspond to either the mature glycosylated form or intermediate glycosylated species. As expected γ_7(1-217) and γ_7(1-238) were not detected by the γ_7(C-terminal tail) Ab. The specificity of the Abs is indicated by the lack of immunostaining in the absence of transfected constructs (-). Similar results were obtained in *Xenopus* oocytes (data not shown). The same amount of total protein was loaded in each lane (25 μg).

B, Examples of Western blots showing the effect of (i) γ_7, and (ii) γ_7(1-271), and the lack of effect of (iii) γ_7(1-217) and (iv) $K_V3.1b$ on the level of $Ca_V2.2$ protein expressed in Cos-7 cells. Con = transfection with Kir-AAA cDNA, in place of γ_7 (see Methods). The same amount of total protein was loaded in each pair of lanes (25 μg).

C, Correlation between the effect of the γ_7 and its various C-terminal truncated constructs on the level of $Ca_V2.2$ protein with their effect on $Ca_V2.2$ I_{Ba} shown in Fig. 1*C*. The effect of γ_7, γ_7(1-217), γ_7(1-271) and γ_7(1-238) on $Ca_V2.2$ protein levels represents the mean inhibition observed in 3-10 experiments. The linear fit has a correlation coefficient, r, of 0.936. All error bars are s.e.m.

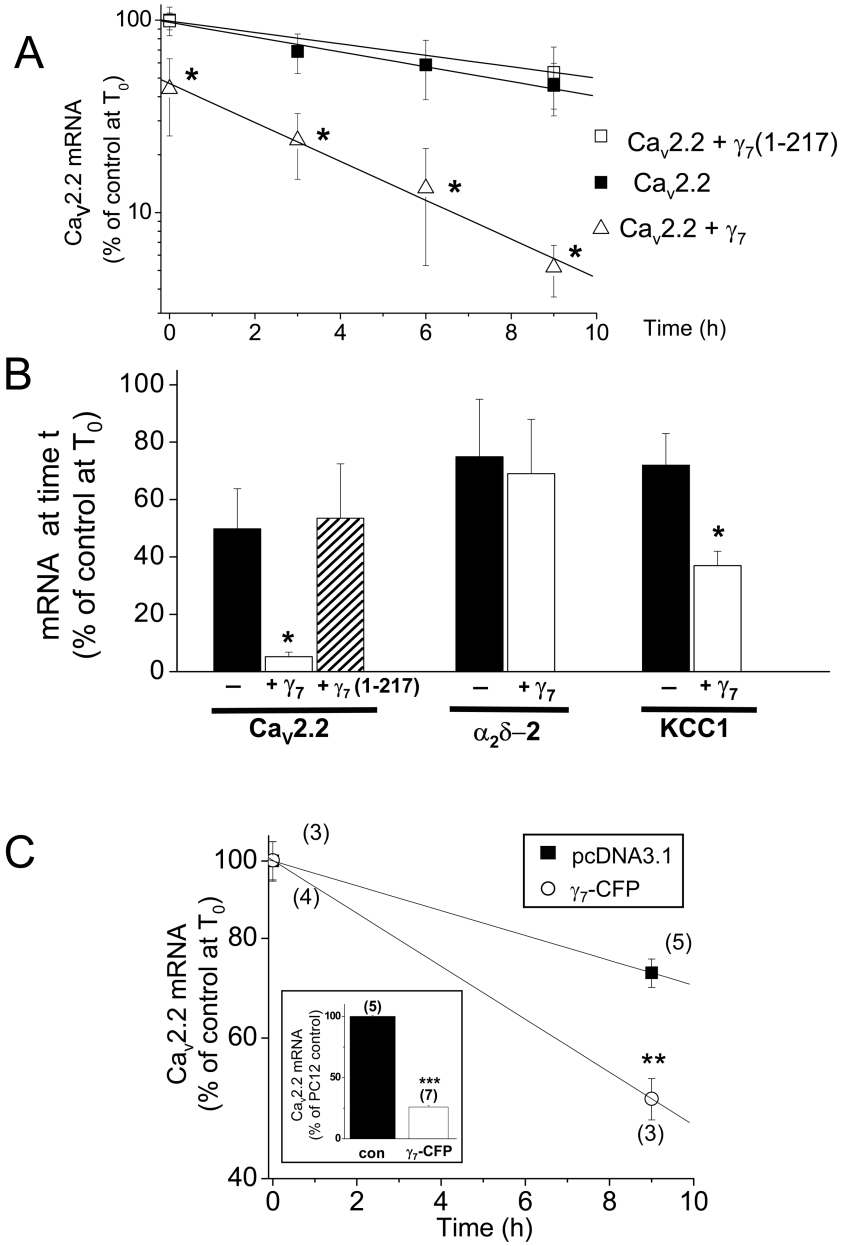

Figure 3. Effect of γ_7 and C-terminally truncated γ_7(1-217) on $Ca_V2.2$ mRNA stability

A, Effect of γ_7 on $Ca_V2.2$ mRNA degradation rate. Constructs were expressed in *Xenopus* oocytes either without (■) or with γ_7 (Δ) or with γ_7(1-217) (□). In the absence of a γ_7 construct, an equivalent amount of a similar sized transcript, a non-functional K^+ channel Kir-AAA cDNA was used. After 24 h (T_0), actinomycin D (50 μg/ml) was added to the medium, and the $Ca_V2.2$ mRNA levels measured at the times shown after this. The numbers of determinations from individual oocytes are between 6 and 12 for each data point; * P<0.05 compared to $Ca_V2.2$ (Student's t test). The lines are apparent linear fits using errors as weight.

B, Bar chart showing the % of $Ca_V2.2$, $\alpha_2\delta$-2 and KCC1 mRNA present at time t after actinomycin D addition at time T_0. For $Ca_V2.2$ mRNA turnover, t = 9 h. Bars 1 - 3 are control (black bar, n = 11); + γ_7, (white bar, n = 7) and +γ_7(1-217) (hatched bar, n = 8).

Bars 4 -7 show the % of $\alpha_2\delta$-2 mRNA and KCC1 mRNA present 9 and 24 h respectively after actinomycin D addition for the control condition (black bar, n = 8 and 9), + γ_7 (white bar, n = 9 and 9). These times were chosen as the % of mRNA remaining in control conditions was similar for all mRNA species. * P<0.05, compared to control, Student's t test.

C, Degradation rate for endogenous $Ca_V2.2$ in the γ_7-CFP PC12 cell line (○, n = 3), compared to control pcDNA3.1-transfected PC12 cell line (■, n = 5), following differentiation with NGF. The $Ca_V2.2$ mRNA level is expressed as % of time 0 (T_0), when actinomycin D was added. The half-life for endogenous $Ca_V2.2$ mRNA was 19.5 h in the pcDNA3.1 transfected PC12 cell line. In γ_7-transfected PC12 cells the half-life was 9.1 h (** P<0.01, Student's t test). **Insert**: Reduction of endogenous $Ca_V2.2$ mRNA level in γ_7-CFP PC12 cell line, compared to control pcDNA3.1-transfected PC12 cell line. *** P<0.001 vs control.

Europe PMC Funders Author Manuscripts

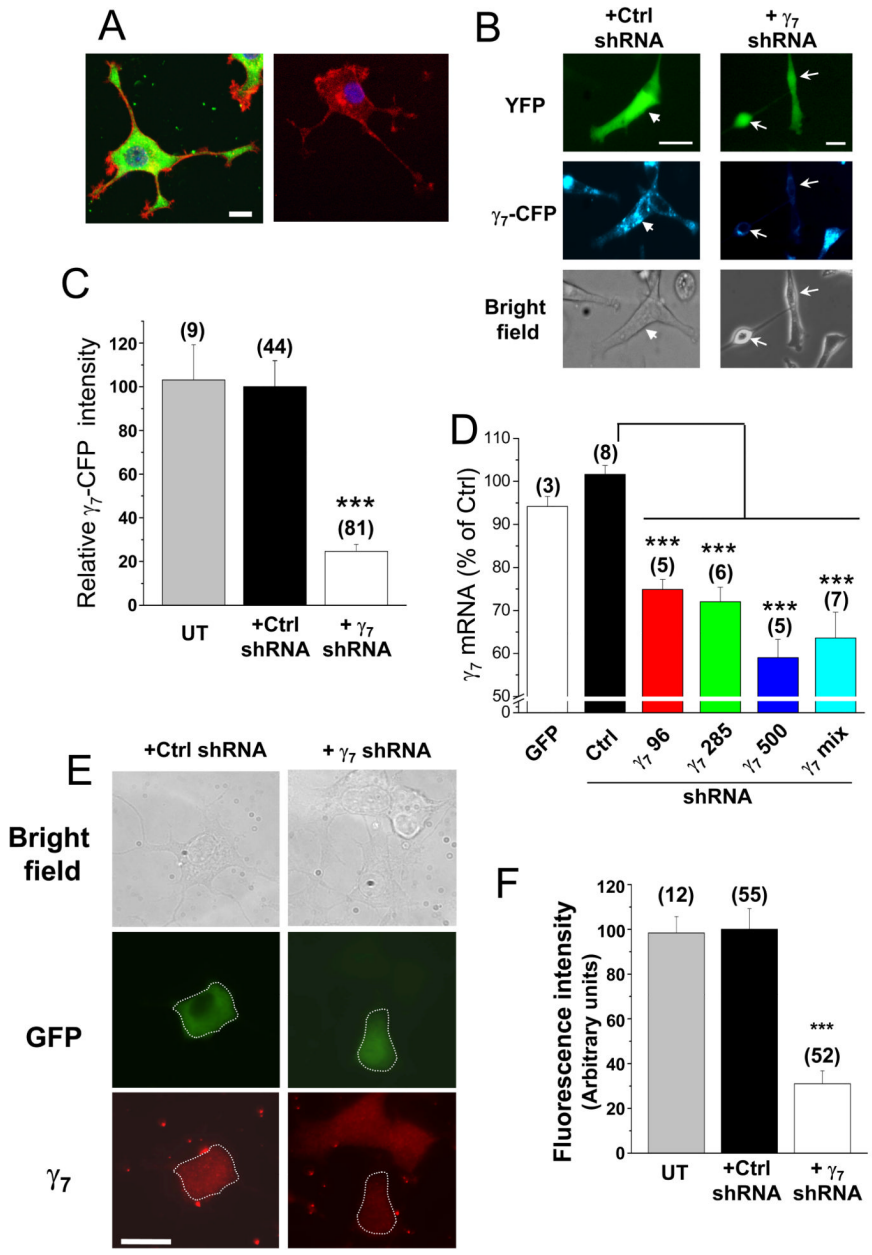

Figure 4. Short hairpin RNA constructs knockdown γ_7 levels in PC12 cells

A, Left: endogenous γ_7 (detected using γ_7 I-II loop Ab, green) in a differentiated PC12 cell, together with F-actin (Alexa Fluor 594-phalloidin, red) and nuclear staining (DAPI, blue). Right: control in the absence of primary γ_7 Ab. Calibration bar 10 μm applies to both images. The images are a Z-stack of 5 to 8 confocal images.

B, Fluorescence microscopy of PC12 cells stably transfected with a human γ_7-CFP construct. These cells were transiently transfected with YFP and either negative control *gnu* shRNA (Ctrl, left panel) or a mixture of three human γ_7 shRNAs (γ_7, right panel), and examined after 5 days. Upper row: transfected cells are identified with YFP fluorescence. Middle row: CFP fluorescence is almost abolished in cells transfected with γ_7 shRNA. Arrowhead in left panel indicates a cell transfected with the control shRNA that shows γ_7-

Europe PMC Funders Author Manuscripts

CFP fluorescence. Arrows in right panel indicate two cells transfected with γ_7 shRNA that do not show γ_7-CFP fluorescence. Lower row: bright field. Scale bars 30 μm.

C, Bar chart of the mean percentage of CFP fluorescence in PC12 γ_7-CFP cells after transfection with γ_7 shRNA (white bar) compared to transfection with Ctrl shRNA (black bar) or untransfected PC12 cells (UT, gray bar). *** $P<0.001$ vs Ctrl.

D, Effect of rat γ_7 shRNA on γ_7 mRNA level in PC12 cells. γ_7 mRNA was quantified by q-PCR in PC12 cells transfected with GFP (white bar), negative control shRNA (Ctrl, black bar) or human γ_7 shRNAs: γ_7 96 (red bar), γ_7 285 (green bar), γ_7 500 (blue bar) or γ_7 mix (cyan bar). *** $P<0.001$ vs Ctrl.

E, Effect of transfection with γ_7 shRNA on endogenous γ_7 protein levels in PC12 cells. Left panel: cells transfected with control shRNA and GFP, right panel: cells transfected with rat γ_7 shRNA and GFP. Top row: bright-field image; middle row: GFP, with transfected cell outlined; bottom row: endogenous γ_7 visualized by immunocytochemistry (red), showing reduced fluorescence in γ_7 shRNA-transfected cell (outlined). Scale bar 20 μm applies to all images, which were taken on a conventional fluorescence microscope.

F, Quantification of data including that given in ***E,*** showing reduction in mean fluorescence intensity (measured as fluorescence density in arbitrary units) in γ_7 shRNA transfected cells (white bar), compared to control shRNA (Ctrl, black bar) or untransfected cells (UT, gray bar); *** $P<0.001$, compared to Ctrl.

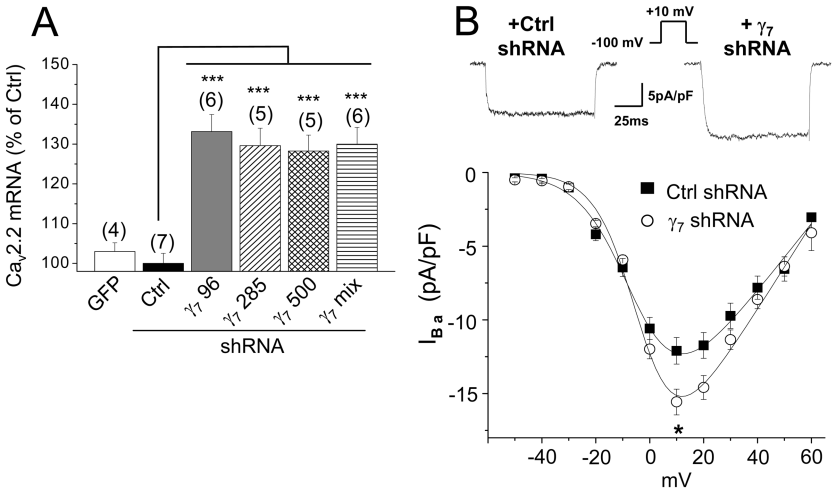

Figure 5. Short hairpin RNA constructs enhance endogenous $Ca_V2.2$ mRNA levels and calcium channel currents in PC12 cells

A, Effect of rat γ_7 shRNA on endogenous $Ca_v2.2$ mRNA level in PC12 cells. $Ca_v2.2$ mRNA was quantified by q-PCR in PC12 cells transfected with GFP (white bar), negative control shRNA (Ctrl, black bar) or γ_7 shRNAs: γ_7 96 (gray bar), γ_7 285 (hatched bar), γ_7 500 (cross-hatched bar) or γ_7 mix (striped bar). *** P<0.001 vs Ctrl.

B, Upper panel: representative traces of peak calcium channel currents recorded from differentiated PC12 cells transfected with Ctrl shRNA (left panel) and γ_7 shRNA (right panel). Currents were elicited by a 100 ms depolarization step to +10 mV from a holding potential of -100 mV. Lower panel: Current-voltage relationships for the two conditions (■, Ctrl shRNA; ○ γ_7 shRNA). The charge carrier was 10 mM Ba^{2+}. The knockdown of γ_7 induces an increase of the peak current (-16.1 ± 0.9 pA/pF, n = 48) compared with control (-12.5 ± 0.9 pA/pF, n = 17, P<0.05).

Europe PMC Funders Author Manuscripts

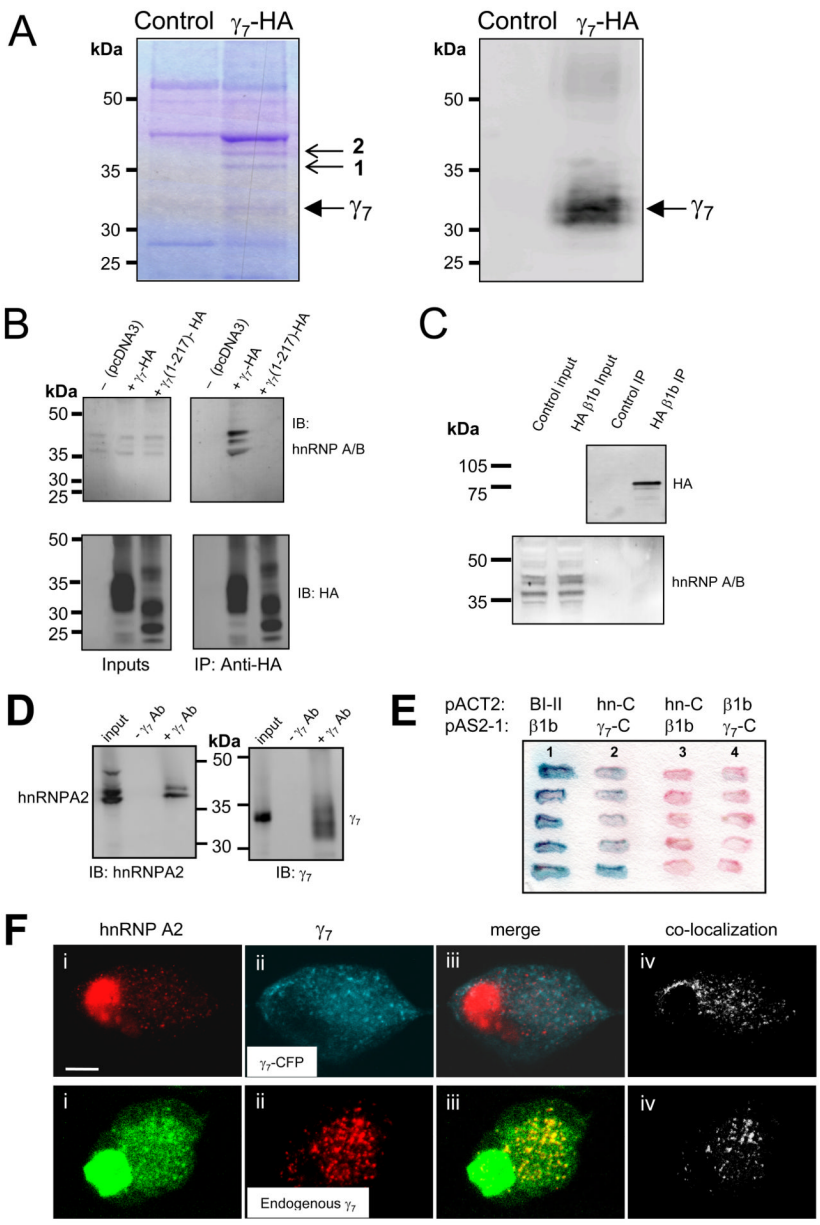

Figure 6. Identification of proteins interacting in a complex with γ_7

A, Proteins co-immunoprecipitated with γ_7-HA from stably transfected PC12 cells. Left: Coomassie staining. Right: western blotting and immunodetection with anti-HA Ab of immunoprecipitated and control samples separated by SDS-PAGE. Solid arrow indicates γ_7-HA. Small arrows indicate proteins co-immunoprecipitated with γ_7-HA. Bands 1 and 2 were identified by peptide mass fingerprinting to contain hnRNP A2. Band 2 also contained hnRNP-A3. The control lane is untransfected PC12 cells. Position of molecular weight markers is shown on the left. Representative of three experiments.

B, Endogenous hnRNP A2 co-immunoprecipitates with transiently transfected γ_7-HA, but not with γ_7(1-217)-HA in tsA-201 cells. Western blotting and immunodetection with anti-hnRNP A/B Ab (H-200, upper row) and anti-HA Ab (lower row) of input (left) and HA-immunoprecipitated samples (following 500 mM NaCl wash, right) separated by SDS-

PAGE. Position of molecular weight markers is shown on the left. Blots are representative of 3 - 5 independent experiments, using anti-hnRNP A/B Abs from two different sources.
C, $Ca_V\beta1b$ with a C-terminal HA tag was expressed and immunoprecipitated as described for γ_7-HA. Its presence in the precipitate is confirmed in the upper blot. The control lane is from cells not transfected with $Ca_V\beta1b$-HA. Immunoblotting for endogenous hnRNP A2 shows it is present in the input lanes, but absent from the immunoprecipitate.
D, Co-immunoprecipitation of endogenous hnRNP A2 and γ_7 proteins from PC12 cells. Western blotting and immunodetection with anti-hnRNP A2 Ab (EF67, left panel) and γ_7 C-terminus Ab (right panel) of input (left-hand lane of both panels) and γ_7 C-terminus Ab-immunoprecipitated samples (right-hand lane of both panels) separated by SDS-PAGE. Control immunoprecipitations where γ_7 Ab was omitted are shown in the center lane of each panel. Position of molecular weight markers is indicated between the panels. Blots are representative of 2 independent experiments.
E, The interaction of the C-terminus of hnRNP A2 with the cytoplasmic C-terminal tail of γ_7 was independently confirmed by yeast co-transformation tests. Lane 1: positive control (blue reaction product) showing $Ca_V2.2$ I-II loop (BI-II) pACT2 and β1b pAS2-1. Lane 2: interaction between hnRNP A2 C-terminus (hn-C) in pACT2 and γ_7 C-terminus (γ_7-C) in pAS2-1. Lanes 3 and 4: negative controls showing that the hnRNP A2 C-terminus and the γ_7 C-terminus do not interact with β1b in the alternative vector. The filter was incubated with the X-gal (5-bromo-4-chloro-3-indolyl-b-D-galactopyranoside) substrate for 5h.
F, Regions of co-localization of hnRNP A2 with γ_7-CFP (upper row), or endogenous γ_7 (lower row) in SCG neurons. Panel i: immunolocalization of endogenous hnRNP A2 in SCG neuron cell bodies (upper panel, red; lower panel, green). Panel ii: localization of γ_7-CFP (upper panel, blue) or immunolocalization of endogenous γ_7 (lower panel, red). Panel iii: merger of images of i and ii, with the co-localized regions shown in white (upper panel) or yellow (lower panel). Panel iv: co-localized γ_7 and hnRNP A2 pixels are also shown separately for clarity (white). Scale bar 10 μm applies to all images. No endogenous γ_7 staining was observed in the absence of primary Ab (data not shown).

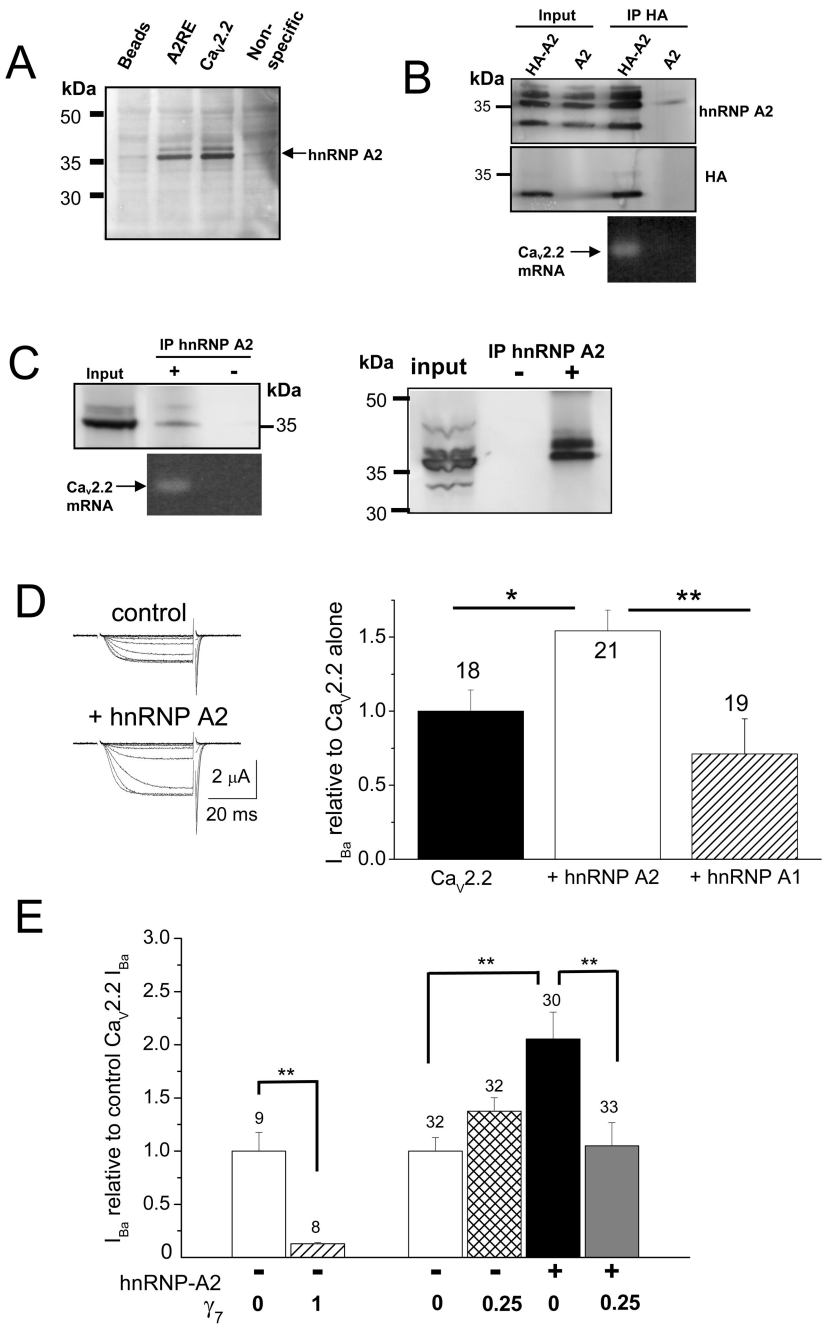

Figure 7. Binding of hnRNP A2 to $Ca_V2.2$ mRNA and effect of hnRNP A2 and γ_7 on $Ca_V2.2$ currents

A, Evidence that one of the two potential A2RE sites in $Ca_V2.2$ mRNA binds to hnRNP A2. Endogenous hnRNP A2 (indicated by the arrow) from mouse brain lysate was pulled down by biotinylated oligonucleotides containing the consensus A2RE site (lane 2) and the potential site in $Ca_V2.2$ (lane 3) but not by beads alone (lane 1) or by a non-specific sequence with the same composition as the consensus A2RE site (lane 4). The hnRNP A2 was detected by immunoblotting with anti-hnRNP A2 Ab (F16). Position of molecular weight markers is shown on the left. Representative of two experiments.

Europe PMC Funders Author Manuscripts

B, Coimmunoprecipitation of endogenous $Ca_V2.2$ mRNA associated with hnRNP A2 in PC12 cells. Two days after transfection with HA-hnRNP A2 (HA-A2, lanes 1 and 3) or hnRNP A2 (A2, lanes 2 and 4), hnRNP A2 protein was immunoprecipitated from the whole cell lysate (lanes 1 and 2) with HA antibody (lanes 3 and 4). Immunoblots show that HA Ab pulled-down hnRNP A2 (top row, anti-hnRNP A2 (EF-67 Ab); middle row, anti-HA). Co-immunoprecipitated RNA was extracted, reverse transcribed and amplified by PCR. A specific PCR product corresponding to the endogenous $Ca_V2.2$ mRNA was amplified (35 cycles) only in the condition where hnRNP A2 protein was pulled-down (bottom row, lane 3).

C, Left panel: Endogenous hnRNP A2 proteins were immunoprecipitated from PC12 cells with anti-hnRNP A2 Ab EF-67 (upper row, lane 2). In this condition, a specific PCR product corresponding to the endogenous $Ca_V2.2$ mRNA was also amplified (35 cycles, lower row). $Ca_V2.2$ mRNA was not detected in the control where antibody was omitted (lane 3). Right panel: The immunoprecipitation was repeated, including an acetone precipitation step, to confirm the presence of endogenous hnRNP A2.

D, Enhancement by hnRNP A2 but not hnRNP A1 of $Ca_V2.2$ currents recorded from *Xenopus* ooctyes. Left panel: example traces elicited by 50 ms step depolarizations to between -40 and 0 mV in 10 mV steps, from a holding potential of -100 mV for $Ca_V2.2/\beta1b/\alpha_2\delta$-2 (upper traces) or $Ca_V2.2/\beta1b/\alpha_2\delta$-2 plus hnRNP A2 (lower traces). The charge carrier was 10 mM Ba^{2+}. Right panel: bar chart shows the effect of hnRNP A2 co-expression with $Ca_V2.2/\beta1b/\alpha_2\delta$-2 on peak $Ca_V2.2$ I_{Ba} amplitude, expressed relative to the mean peak control current in each experiment. Control (black bar, n = 18), for both groups taken from experiments directly comparing hnRNP A1 and hnRNP A2: + hnRNP A2 (white bar, n = 21) and + hnRNP A1 (hatched bar, n = 19). These data are pooled from two separate experiments showing similar results. Statistical significance * $P<0.05$, ** $P<0.01$ (one way ANOVA and Bonferroni's post test).

E, Inhibition of the hnRNP A2-mediated enhancement of I_{Ba} in *Xenopus* oocytes by a low concentration of γ_7. Bar chart compares the effect of two concentrations of γ_7 cDNA (γ_7: $Ca_V2.2$ ratio 1 and 0.25), and also shows the lack of enhancement by hnRNP A2 on peak $Ca_V2.2$ I_{Ba} amplitude, when co-expressed with the lower concentration of γ_7 (γ_7: $Ca_V2.2$ ratio 0.25). Data are expressed as a % of the mean peak control $Ca_V2.2$ current in each experiment, and all data were recorded 2 days after cDNA injection. Control in the absence of γ_7 or hnRNP A2 (white bars); + γ_7 (ratio 1; hatched bar), + γ_7 (ratio 0.25; cross-hatched bar) + hnRNP A2 (black bar, from data obtained in the same experiments), + hnRNP A2 and γ_7 (ratio 0.25) (gray bar). Number of determinations given above each bar. These data are pooled from 5 different batches of oocytes, in all of which similar results were observed. Statistical significance ** $P<0.01$ (one way ANOVA and Bonferroni's post test).

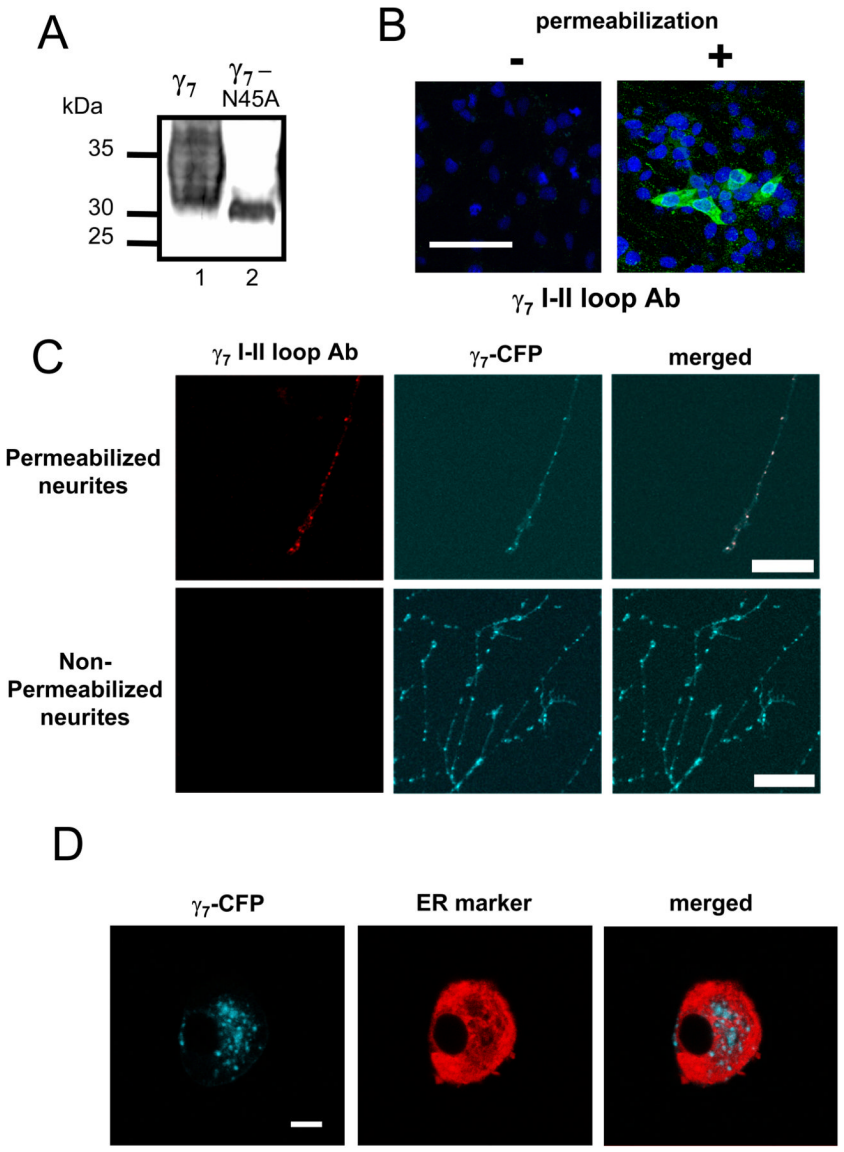

Figure 8. Subcellular localization of γ_7

A, Western blotting of a γ_7 mutant in which the potential glycosylation site, N45 is mutated to A, and immuno-detection with anti-γ_7 I-II loop Ab. Lane 1: γ_7; lane 2: γ_7N45A. The reduction in mass and sharpening of the band indicates that γ_7 is normally glycosylated at this site. Positions of molecular weight markers are shown on the left. The data are representative of 2 independent experiments.

B, Immunodetection of transiently transfected γ_7 (green) in non-permeabilized (left) and permeabilized (right) tsA 201 cells, using γ_7 I-II loop Ab. The nuclear stain DAPI (blue) was used as a cell marker. Scale bar: 100 μm, applies to both images. No immunostaining was observed in any field in the absence of permeabilization.

C, Immunostaining for γ_7 using I-II loop Ab (Texas red secondary Ab, left panel) co-localizes completely with γ_7-CFP (middle panel), as shown by yellow regions in merged image (right), in permeabilized (upper row), but not non-permeabilized (lower row) SCG neurons. Scale bar: 40 μm, applies to all images.

D, Partial co-localization of γ_7-CFP and an ER marker in SCG neurons. Left: γ_7-CFP; center: ER marker (ER-DsRed), right: overlay showing co-localization of DsRed with γ_7-CFP (white). Scale bar: 10 μm and applies to all images.

Europe PMC Funders Author Manuscripts

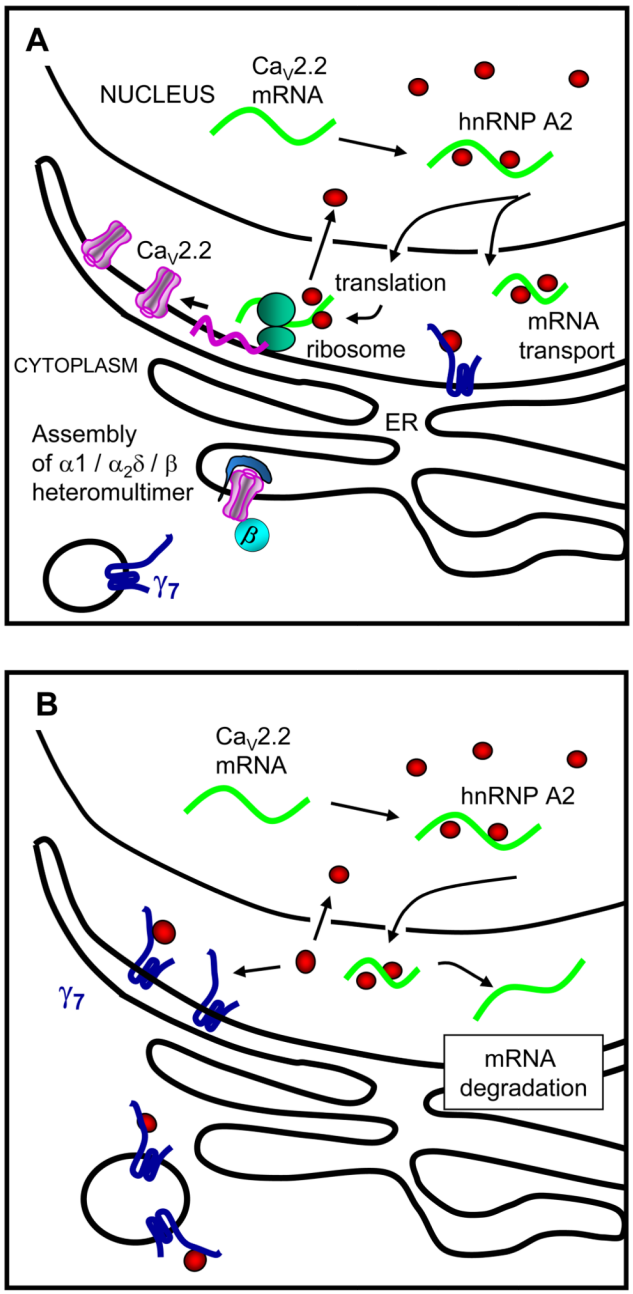

Figure 9. Diagram of proposed function of γ_7

A, The physiological distribution of hnRNP A2 and γ_7. The hnRNP A2 (red circles) is localized largely in the nucleus where it binds to A2RE sequences on mRNAs and exits to the cytoplasm with these mRNAs, including that of $Ca_V2.2$ (green). This is thought to stabilize certain mRNAs, reducing degradation and therefore enhancing expression. Our results suggest this may be the case for $Ca_V2.2$. hnRNP A2 may also stabilize the mRNAs for transport. γ_7 (dark blue) is present on the ER and is also associated with motile vesicles. ***B,*** Following overexpression of γ_7, it may sequester cytoplasmic hnRNP A2 and therefore increase degradation of $Ca_V2.2$ mRNA.

Europe PMC Funders Author Manuscripts

Table 1

hnRNP A2 mRNA binding motifs in $Ca_V2.2$ mRNA

	sequence	similarity to consensus sequence in MBP	Gene
MBP A2RE	GCCAAGG**AG**CCAGAGAGCAUG	21 bases = A2RE	
(1) $Ca_V2.2$ rabbit	GCUAAGG**AG**CGCGAGAGAGUG	16/21 identical	*Cacna1b* Exon 9
mouse	GCCAAGG**AG**CGGGAGCGAGUC	15/21 identical	
human	GCCAAGG**AG**CGAGAGAGGGUG	18/21 identical	
(2) $Ca_V2.2$ rabbit	UCCAAGG**AG**CUGGAGCGTGAC	13/21 identical	*Cacna1b* Exon 27
mouse	UCCAAGG**AG**CUGGAGAGGGAC	14/21 identical	
human	UCCAAGG**AG**CUGGAGAGGGAC	14/21 identical	

The binding motif identified in MBP (Hoek et al., 1998) is compared to the two found in $Ca_V2.2$. The essential conserved AG bases are in bold and the sequences identical to MBP A2RE are underlined. Exon numbering as shown in ENSEMBL.